Proton NMR Relaxometry as a Useful Tool to Evaluate Swelling Processes in Peat Soils

Fabian Jaeger[a], Anastasia Shchegolikhina[b], Henk Van As[c] and Gabriele Ellen Schaumann*[,a]

[a]*Department of Environmental and Soil Chemistry, Institute of Environmental Sciences, Universität Koblenz-Landau, Fortstr. 7, 76829 Landau, Germany*

[b]*Geographical Institute, Ruhr-University Bochum, Universitaetsstrasse 150, 44801 Bochum, Germany.* [c]*Laboratory of Biophysics and Wageningen NMR Centre, Dreijenlaan 3, 6703 HA Wageningen, The Netherlands*

Abstract: Dramatic physical and physico-chemical changes in soil properties may arise due to temperature and moisture variations as well as swelling of soil organic matter (SOM) under constant conditions. Soil property variations may influence sorption/desorption and transport processes of environmental contaminants and nutrients in natural-organic-matter-rich soils. Notwithstanding the studies reported in literature, a mechanistic model for SOM swelling is unavailable yet. The objective of the present study was the evaluation of the swelling of peat soils, considered as SOM models, by ^{1}H NMR relaxometry and differential scanning calorimetry (DSC). Namely, information on the processes governing physical and physicochemical changes of peat during re-hydration were collected. The basic hypothesis of the present study was that the changes are slow and may affect water state as well as amounts of different water types into the peats. For this reason, such changes can be evidenced through the variations of mobility and thermal behaviour of the involved H_2O molecules by using ^{1}H NMR relaxometry and DSC. According to the experimental results, a mechanistic model, describing the fundamental processes of peat swelling, was obtained. Two different peats re-wetted at three temperatures were used. The swelling process was monitored by measuring spin-spin relaxation time (T2) over a hydration time of several months. Moreover, DSC, T1 – T2 and T2 – D correlation measurements were done at the beginning and at the end of the hydration. Supplementary investigations were also done in order to discriminate between the swelling effects and the contributions from soil solution, internal magnetic field gradients and/or soil microorganisms to proton relaxation. All the results revealed peat swelling. It was evidenced by pore size distribution changes, volumetric expansion and redistribution of water, increasing amounts of nonfreezable and loosely bound water, as well as formation of gel phases and reduction of the translational and rotational mobility of H_2O molecules. All the findings implied that changes of the physical and physicochemical properties of peats were obtained. In particular, three different processes having activation energies comprised in the interval 5 – 50 kJ mol^{-1} were revealed. The mechanistic model which was, then, developed included water reorientation in bound water phases, water diffusion into the peat matrix and reorientation of SOM chains as fundamental processes governing SOM swelling. This study is of environmental significance in terms of re-naturation and re-watering of commercially applied peatlands and of sorption/desorption and transport processes of pollutants and nutrients in natural organic matter rich soils.

Keywords: Soil organic matter, swelling, kinetics, unfreezable water, differential scenning calorimetry, NMR relaxometry, pore water.

INTRODUCTION

Natural soils are exposed to dynamic variations in temperature and moisture. Changes in moisture status may affect soil properties like water content or volumetric swelling of soil organic matter (SOM) [1, 2] or sorbent properties [2-5]. Furthermore, the extractability of organic pollutants was found to be affected by the hydration time of soils indicating physical and physicochemical changes of SOM upon swelling [2]. Although it is known that SOM swelling includes volumetric expansion [1], water redistribution and re-opening of small-sized pores [6] as well as SOM re-organisation [7, 8] a mechanistic model describing the fundamental processes of SOM swelling is not available until now.

Peat soils may be considered as concentrated analogues of SOM, and, therefore, they were used as models for environmental studies of pollutant sorption and transport in SOM [9]. Peats are the product of accumulation and humification of plant material in certain special wet habitats [7, 9], and are commercially used as fuel and horticulture medium [7].

Beside peats, many macromolecular substances, such as synthetic polymers or biopolymers, swell when placed in contact with fluids. The swelling is characterised as sorption of the liquid into the macromolecular solid phase, which in turn, increases its volume. This volumetric swelling, *Q*, was defined as the ratio of swollen to non-swollen volume of the sorbent or macromolecular material; a value of unity indicates no swelling. The amount of swelling depends both on the nature of fluid and sorbent. Strongly cross-linked materi-

*Address correspondence to this author at the Department of Environmental and Soil Chemistry, Institute of Environmental Sciences, Universität, Koblenz-Landau, Fortstr. 7, 76829 Landau, Germany; Tel: +49(6341) 280-571; Fax: +49(6341) 280-576; E-mail: schaumann@uni-landau.de

1874-7698/10

als swell less than weakly cross-linked materials. However, swelling seems to be limited by molecular size exclusion effects to fairly small liquid molecules with molar volumes smaller than about 93 cm^3 mol^{-1} for most soil organic materials and 88 cm^3 mol^{-1} for cellulose. The *Q* values for different materials after water sorption ranged between 1.3 and 1.6 for peat, 2.0 for cellulose and 1.6 for chitin. [1]

Unlike synthetic polymers, McBrierty *et al.* [7, 8] reported that the peat matrix re-organises during swelling, thereby permitting access to a greater number of water molecules to the hydrophilic sites. Furthermore, up to four different types of water in hydrated peat samples were identified using differential scanning calorimetry (DSC), thermogravimetric analysis (TGA) and proton nuclear magnetic resonance (NMR) relaxometry. They differentiated between tightly bound or non-freezable water, up to two types of loosely bound or freezable water and freezable bulk water. Non-freezable water is predominantly hydration water and/or water that interacts chemically with hydrophilic moieties in the matrix showing glassy behaviour with a transition temperature around -123°C to -83°C [7]. The character of loosely bound water deviates less dramatically from that of normal water. This water melts with further increase in temperature, but at lower temperatures than freezable bulk water that melts around 0°C [7, 10]. In hydrogels, at least three kinds of water were determined: hydrated water, interfacial water, with a certain ordered arrangement, and bulk water [11].

Additionally to the calculation of *Q*, ^{1}H NMR relaxometry [2, 6, 7, 12, 13] and DSC [7, 14] were used to study the hydration of peat and mineral soil samples or to characterise different types of water in peats. DSC was used to study the melting and freezing behaviour of water and to calculate the amounts of non-freezable and freezable water in hydrogels [15, 16] or peat soil samples [7, 14]. The melting of freezable water in moist samples is characterised by endothermic water melting peaks in the DSC thermograms, which originate from the additional energy uptake of the melting process. The enthalpies of these peaks are often smaller than it would be expected regarding the amount of water present in the samples, which is due to the existence of non-freezable water. In general, the melting peaks of water in hydrogels and peat differ strongly from those of free pure water or solutions. They are broader and split into two or more overlaying peaks. Radosta and Schierbaum found a splitting of the melting peak of water only in maltodextrin gels, but not in maltodextrin solutions, although the determined amounts of non-freezable water were comparable for both systems [15, 17]. Consequently, they attributed the melting peak splitting to the entrapment of water within the gel matrix. In peat soil samples, the splitting of the melting peak was ascribed to the existence of loosely bound and freezable bulk water [7, 14].

Swelling kinetics experiments of soil samples using ^{1}H NMR relaxometry have shown that the swelling process is linked to the migration of the peak relaxation times towards smaller relaxation times and the increase of the amount of water protons relaxing at smaller relaxation times [2, 6, 12, 13]. These findings were attributed to a redistribution of water during swelling. Todoruk *et al.* [6] identified two processes with time constants of about 1 d for a fast process and up to 22 d for a slow process for different soils, which were comparable to the values reported by Schaumann *et al.* [2, 12] and Jaeger *et al.* [13]. The calculated activation energies of these two processes ranged from 14 kJ mol^{-1} to 117 kJ mol^{-1} suggesting diffusion processes and chemical reactions, such as ester hydrolysis [6]. The slow process was attributed to the formation of gel phases and to the slow water intrusion into micropores, which re-opened during swelling.

The changes in the relaxation time distributions during swelling of soils were found to be pronounced stronger in soils with higher microbial respiratory activity [13] and in soils inoculated with a biofilm producing bacteria isolate [18]. Consequently, soil microorganisms may contribute to the swelling of soils due to the production and release of extracellular polymeric substances (EPS) and the formation of biofilm. Furthermore, the proton relaxation in soil solutions (bulk relaxation) may significantly contribute to the total proton relaxation of water in soil samples and the contribution of the bulk relaxation may increase during hydration due to dissolution of paramagnetic iron and manganese or changes of their chemical speciation [19]. Keating and Knight [20] found for iron-oxide coated sands that some of the studied surface species of iron produced internal field gradients causing additional transverse proton relaxation due to spin diffusion in internal field gradients at 2.2 MHz. Thus, a contribution of this additional transverse proton relaxation mechanism cannot be excluded a priori for hydrated soil samples measured at lower magnetic field strength.

In general, transverse relaxation times (T_2) are used to study the swelling of soil samples [6, 12, 13], because of the much faster determination compared to longitudinal relaxation times (T_1). However, many swellable materials, such as cellulose [21], hydrogels with different degrees of cross-linking [22], wheat starch [23] and maltodextrin [17] show strong differences between T_1 and T_2. Their T_1/T_2 ratios were found to be much larger than for free pure water ($T_1/T_2 \sim 1$) or for rock core samples with T_1/T_2 ratios generally between 2 to 3 [24]. The larger T_1/T_2ratios in those swellable materials were attributed to a water structuring caused by the polymer, which resulted in reduced rotational mobility of water molecules inside the structured water phase [17]. This reduced rotational mobility affects T_1 and T_2 differently [25]. The structured water is non-freezable water [26, 27] that exchanges very fast with the bulk water phase, which results in only one average relaxation time much smaller than for bulk water [23]. In starch pastes, the T_1/T_2 ratio of the bound water was found to be 22 and the one determined from the average relaxation times was about 8 [23]. As a consequence, both T_1 and T_2 measurements may be helpful to investigate water mobility and a possible structuring of water caused by the SOM matrix in swollen soils.

We hypothesised that the physical and physicochemical properties of peat soil samples change during volumetric swelling at constant temperature and moisture conditions. These changes are slow and affect the state of water as well as the amounts of different water types inside the peats. Thus, they can be observed through changes in mobility and thermal behaviour of the involved water molecules, which

can be determined by ^{1}H NMR relaxometry and DSC. Our objectives were to study the swelling of peat soils *via* ^{1}H NMR relaxometry and DSC to characterise the governing processes causing physical and physicochemical changes of peat during re-hydration at constant temperature and moisture conditions. For that we have combined T_1 and T_2 measurements together with DSC measurements for the first time to study the swelling of peat soil samples. Swelling kinetics experiments were carried out with two re-wetted peats at three different temperatures. Additional investigations were carried out to distinguish between swelling effects and further influences on the proton relaxation process caused by the soil solution, internal magnetic field gradients and/or soil microorganisms.

MATERIALS AND METHODOLOGY

Peat Soil Samples

The peat material used in this study was taken from the peat land "Totes Moor" in the nature park "Steinhuder Meer" near Hannover, Germany. The samples of peat were collected from the drained part of the bog from two different layers: a fibric peat (peat 1) was collected from an upper layer with low degree of decomposition and a well decomposed sapric peat (peat 2) was taken from 1.1 m depth. After sampling, the peats were air dried at room temperature and characterised (Table **1**). For NMR measurements, the air dried peat samples were ground, 2 mm sieved and stored at 19°C until further usage.

Table 1. Description and Some Properties of the Two Studied Peat Soil Samples. CEC_{eff} Effective Cation Exchange Capacity. DOC Dissolved Organic Carbon. $wc_{air\ dried}$ Gravimetric Water Content of the Air Dried Peat Samples Related to Dry Mass (d.m.) Determined after Oven Drying for 24 h at 105°C

	Fibric Peat	**Sapric Peat**
Label	**Peat 1**	**Peat 2**
Color	**Brown**	**Black**
Sampling depth /m	0.4	1.1
Ash-content /%	1.25	1.28
pH ($CaCl_2$ 0.01 M)	2.7	2.7
C_{org} /%	45	52
C/N	405	219
DOC /mg L^{-1}	89	56
CEC_{eff} /$mmol_c$ kg^{-1}	166	123
$wc_{air\ dried}$ /g g d.m.	0.152	0.161
Sampling coordinates	52° 30' 26.41" N 9° 21' 14,28" E	

^{1}H NMR Relaxation in Porous Media

In porous materials, the proton relaxation is strongly accelerated by interactions between water protons and surfaces [detailed information can be found in e.g. 12, 28-30]. As a result, the measured relaxation time of water protons is determined by the proton relaxation time in the pore space, $T_{1,2B}$, the surface relaxation time, $T_{1,2S}$, and the diffusion relaxation time, T_{2D}, due to spin diffusion in internal magnetic field gradients, which affects the transverse proton relaxation time (T_2), but not the longitudinal proton relaxation time (T_1) [28, 31].

$$\frac{1}{T_1} = \frac{1}{T_{1B}} + \frac{1}{T_{1S}} = \frac{1}{T_{1B}} + \frac{\rho_1 S}{V} \quad (1)$$

$$\frac{1}{T_2} = \frac{1}{T_{2B}} + \frac{1}{T_{2S}} + \frac{1}{T_{2D}} = \frac{1}{T_{2B}} + \frac{\rho_2 S}{V} + \frac{1}{T_{2D}} \quad (2)$$

With $SV^{-1} = \alpha r^{-1}$ the proton relaxation time is connected to the pore diameter, $d_{pore} = 2r$, where r is the pore radius and $\alpha = 1$, 2, or 3 is the shape factor for planar, cylindrical, and spherical pore geometry, respectively [32]. SV^{-1} is the pore surface to pore volume ratio, $\rho_{1,2}$ is the surface relaxivity, which is strongly affected by paramagnetic ions on the surface like Mn(II) [33] and Fe(III) [34]. T_{2D} is related to the average internal gradient of the magnetic field, G, and the self-diffusion coefficient of water, D, by

$$\frac{1}{T_{2D}} = \frac{D}{12}(\gamma G t_E)^2, \quad (3)$$

where γ is the gyromagnetic ratio, and t_E is the echo time, which is the time between two 180° pulses in the Carr-Purcell-Meiboom-Gill (CPMG) pulse sequence [35].

Eq. 1 and 2 are valid if the condition for the *fast-diffusion regime*, $\frac{\rho_2 V}{SD} << 1$ is fulfilled [31]. This means that the relaxation process is surface-limited and the diffusion of water protons towards the surface is very fast and can therefore be neglected. Various rock core samples, e.g. sandstones [28, 36], were assigned to the *fast-diffusion regime* [31], whereas some sandy soil samples [37] were in the transition from the *intermediate-* to the *slow-diffusion regime* [31]. However, it has been shown that Eq. 2 can be also used for the calculation of pore sizes in soils by assuming the *fast-diffusion regime* in these soil samples and by using two surface relaxivities for each soil, one for micro- and one for mesopores, [37].

Sample Preparation and ^{1}H NMR Measurements

Sample Preparation

1.00 g dry mass (d.m.) of peat 1 and 3.55 g d.m. of peat 2 of the air dried samples were filled in glass vessels and rewetted to their maximal water holding capacity (i.e. maximal water content). The maximal water content was 15.67 g g^{-1} d.m. for peat 1 and 4.51 g g^{-1} d.m. for peat 2. Thus, the total amount of water was with 15.67 g (peat 1) and 16.01 g (peat 2) comparable for the two rewetted peats.

The protocol of the rewetting procedure was the same for all studied peat samples: After placing the air dried peat sample into the glass vessel, the water (demineralised water) was added and the peat was carefully mixed with the water

using a thin spatula. After wetting of all surfaces, i.e. the peat surfaces turned dark and no dry areas were observed, the vessel was sealed with a plastic lid and knocked ten times vertically on a solid surface to obtain comparable bulk densities. After centrifugation at 4000 RPM at the beginning and end of swelling (see below), the contact angle of the peat samples was determined using the sessile drop method described by Diehl and Schaumann [38] to test the wettability of the surfaces. Before starting the rewetting procedure, both the peat sample and the water were adjusted to the respective temperature of 5°C, 19°C or 30°C. In the course of swelling of 5 to 7 months (hydration time), the sealed glass vessels were stored in desiccators with 99.9 % relative humidity in darkness at the respective temperature (± 1.5°C).

Swelling Kinetics at 5°C, 19°C and 30°C by ^{1}H NMR Measurements

All one-dimensional ^{1}H NMR measurements to determine the swelling kinetics, the water distribution versus centrifugation speed as well as the amounts of unfrozen water at -34°C and -5°C were performed at a magnetic field strength of 0.176 T, i.e. at a proton Larmor frequency of 7.5 MHz (Minispec 7.5, Bruker, Germany). The temperatures during the measurements were kept constant (± 0.5°C) using a XR401 Air-Jet^{TM} sample cooler (FTS Systems, Stone Ridge, USA) with compressed air as gas stream. The relaxation time distributions were determined using a MATLAB program developed by Veevaete [39] applying the BRD (Butler, Reeds and Dawson) algorithm [40]. The relaxation time distributions consisted of 200 time constants (*TC*) with associated amplitudes. The sum of the amplitudes equals the total NMR signal intensity at time $t = 0$ ($SI_{t=0}$), which is a measure of the total amount of water protons in a sample. All one-dimensional ^{1}H NMR measurements were performed with duplicates of the respective peat samples. In this study, we present the results of the two repetition samples (RS 1 and RS 2) separately, because the reproducibility between the duplicates was partly not given.

The two-dimensional T_1 - T_2 and T_2 - D correlation measurements were performed at a proton Larmor frequency of 30 MHz at 20 ± 1°C using a home-made NMR spectrometer controlled by a MARAN Ultra console (Resonance Instruments Ltd, Oxfordshire, UK) with an additional pulsed field gradient (PFG) unit. For T_1 - T_2 correlated measurements the inversion recovery method was combined with a CPMG sequence. 25 steps of the inversion recovery time between 750 µs and 15 s were used to sample a T_1 relaxation decay curve. In the T_2 - D correlation measurement a diffusion-weighted multi-spin-echo pulse sequence [41] was used to determine the correlation between T_2 and the self-diffusion coefficient of water in the peat samples. 25 gradient steps with a maximal gradient strength of 1.2 T m^{-1} were used. Small and big delta were 1 ms and 10 ms, respectively. Two-dimensional T_1 - T_2 and T_2 - D correlation was analyzed by 2D ILT – two-dimensional numerical inverse Laplace transformation [42-44].

The longitudinal relaxation time (T_1) distributions of water in the peat soil samples were determined using an inversion recovery (IR) sequence with 25 IR-points between 1.0 ms and 19 s. Because of the long measurement time for T_1 of about 75 min, the T_1 distribution was only determined direct after water addition (after 110 - 180 min) and at the end of the swelling experiment after 5 to 7 months. A CPMG pulse sequence [35] with an echo time of 500 µs and 50,000 echoes was used to obtain transverse relaxation time (T_2) distributions of water in the peat soil samples in the course of peat swelling. A total of 30 to 36 T_2 measurements were performed to follow the peat swelling over 5 to 7 months. During the first 30 minutes after water addition, T_2 measurements were performed every five minutes. Within the first three to seven hours after water addition, a total of up to eight T_2 measurements were performed to determine fast changes in the T_2 distributions. The effect of the additional transverse relaxation due to spin diffusion in internal field gradients was tested according to Keating and Knight [20] determining T_2 as a function of increasing echo times (500 to 800 µs).

Cryo - NMR Relaxometry: Determination of Non-Freezable and Loosely Bound Water

^{1}H NMR relaxometry experiments at -34°C and -5°C were carried out to determine the amounts of water that were left unfrozen in the peats at these temperatures. The first represents the lowest temperature that was reachable in the peats using the Air-Jet^{TM} sample cooler. The unfrozen water at -34°C is referred to as tightly bound or non-freezable water [7] in this study. It was tested by DSC whether this water remained unfrozen between -90°C and -34°C. From DSC it was found that melting of soil solution extracted from the hydrated peats started above -4°C. Thus, the second temperature of -5°C was operationally chosen to measure the amounts of loosely bound water in peat [7]. This kind of NMR measurement at low temperatures is referred to as Cryo - NMR relaxometry hereafter. The amounts of these two types of water in peat were determined from the NMR signal intensity using a T_2 Hahn-echo [45] sequence with 25 echo points with increasing echo times between 0.05 ms and 7.5 ms at the beginning and end of peat swelling. T_2 of non-freezable and loosely bound water was calculated by mono-exponential fitting to the decay curves determined at -34°C and -5°C, respectively. The wet peat samples were first cooled down to -34°C inside the NMR probe using the Air-Jet^{TM} sample cooler. The freezing process of water was characterised by a dramatic decrease of the NMR signal intensity, because the very short T_2 of ice of about 10 µs [46] could not be detected due to the dead time of 50 µs of the used NMR device. The signal intensity was constant after about 60 min of cooling and the Cryo-NMR measurement was carried out. After that the sample was adjusted to -5°C until constant signal intensity was observed and subsequently measured. Two additional samples (prepared as described above) were used to determine the non-freezable and loosely bound water at the beginning of peat swelling. For the determination of both water types at the end of swelling, the original samples from the swelling kinetics at 30°C were used.

Water Distribution Versus Centrifugation Speed

The water distribution in the peat samples versus centrifugation speed was determined at the beginning and end of swelling and after 2 days of hydration (no repetition sample) using a Universal 320 centrifuge with the rotor 1494 (Het-

tich, Tuttlingen, Germany). The original samples from the swelling kinetics at 30°C were used to determine the water distribution at the end of swelling. Additional repetition samples were used for the determination of the water distribution at the beginning of swelling and after 2 days of hydration. The peat samples were re-wetted as described above and filled into centrifuge tube filters with a 10-µm filter insert (VectaSpin 20, Whatman). Then they were centrifuged step-wise at nine centrifugation speeds between 500 RPM and 4000 RPM for 15 min at 19°C. The peat samples were desaturated during centrifugation. After every centrifugation step, the gravimetric water contents and the T_2 and T_1 distributions of water in the peat samples at 19°C were determined. Instead of the largest T_2 and T_1 in the relaxation time distribution, T_2 and T_1 at 90 % of total sum of amplitudes were determined to reduce variation between replicates [37]. After the last centrifugation step, T_{1B} and T_{2B} were measured in the extracted soil solution, which was gained during centrifugation, to determine the contribution of the soil solution to the total proton relaxation in the wet peat samples.

T_1/T_2 Ratios as a Measure of the Water State in Peat Samples

T_1/T_2 ratios were determined to characterise the state of water in peat samples. For that, we calculated the T_1/T_2 ratios from the relaxation time distributions of water in peat of the fully water saturated samples and the step-wise desaturated samples after centrifugation at the beginning and end of hydration time as a function of the relative water content (*rel. wc*). Relative water contents in the fully saturated samples were calculated from the quotient of the subtotal of the amplitudes (*AT*) of the 200 time constants (*TC*) in a relaxation time distribution and the total sum of the amplitudes ($SI_{t=0}$)

$$rel.wc = \left(\frac{\sum_{i=1}^{200} AT_i}{SI_{t=0}} \right) \times 100. \quad (4)$$

The T_1/T_2 ratios in the saturated samples were determined from *TC* in the T_1 and T_2 distributions at 25 relative water contents between 7.5 % and 100 %. In the desaturated samples, relative water contents were calculated from the quotient of the gravimetric water content after step-wise centrifugation ($wc_{cen.}$) and the total water content at saturation (wc_{tot})

$$rel.wc = \left(\frac{wc_{cent}}{wc_{tot}} \right) \times 100. \quad (5)$$

T_1/T_2 ratios in these samples were determined from T_2 and T_1 at 90 % of total sum of amplitudes after every centrifugation speed (see above).

DSC Measurements

The freezing/melting behaviour of water inside the wet peat samples was studied between -90°C and 40°C using a TA Instruments Model Q1000 DSC (TA Instruments, Alzenau, Germany) with nitrogen as purge gas (50 mL min^{-1}). Heat flow and temperature calibration were carried out using Indium. For the DSC measurements ~3 mg - 10 mg of wet and partly desaturated peat soil from the samples used in the centrifugation experiment were weighed into aluminium pans and hermetically sealed using an aluminium lid. The cooling/heating protocol started with an equilibration at 40°C followed by a cooling cycle down to -90°C with cooling rates of 3 K min^{-1} until -75°C followed by 2 K min^{-1} until -90°C. After equilibration at -90°C, the sample was heated up to 40°C with a heating rate of 5 K min^{-1}. Data analysis (determination of peak onset and peak maximum temperatures, and melting enthalpy) was performed using the Universal Analysis 2000 software by TA Instruments. The peak maximum temperature is referred to as peak position is this study.

According to [14], the melting peak was investigated at four different heating rates between 0.5 K min^{-1} and 10 K min^{-1} to test whether the melting transition is kinetically controlled. For that, the desaturated peat samples from the centrifugation experiment at 4000 RPM, agar gel (30 g L^{-1}), water saturated sand with particle sizes of 150 – 200 µm (referred to as sand 150 µm) and free pure water were used.

The melting enthalpy of freezable water, ΔH_f, in the peat samples as well as the amount of non-freezable water were calculated from the DSC thermograms of the desaturated peat samples from the centrifugation experiment. According to McBrierty *et al.* [7], both were calculated from the integrated change in enthalpy (per gram of dry peat) which was plotted as a function of water content. The slope of a fitted straight line provides ΔH_f and the intercept on the water content axis is the amount of non-freezable water.

Microbial Respiratory Activity

For the incubation experiment the samples were placed in vessels and wetted to 60 % water holding capacity. The rewetted peats (as triplicates) were incubated for 21 days at a temperature of 20°C in a Respicond-apparatus (Nordgren Innovations, Bygdea, Sweden), which determined the CO_2-evolution hourly from the changes in electrical conductivity in 10 ml of 0.6 M KOH solution placed inside the incubation vessels [47].

Calculation of Time Constants and of Apparent Activation Energy the Rate-Limiting Step of Peat Swelling

The T_2 distributions of water in the peat samples used in the swelling kinetics experiment were operationally divided into four T_2 ranges with fixed T_2 limits (I: 0.1 - 3 ms; II: 3 - 30 ms; III: 30 - 300 ms and IV: > 300 ms). The relative amplitudes of the four T_2 ranges were calculated (i.e. the sum of amplitudes of the respective T_2 range divided by the total sum of amplitudes or $SI_{t=0}$) and plotted as a function of hydration time. Previous studies have shown that swelling kinetics of soil samples can be described by first-order processes using exponential functions [12, 13]. We tested fittings with up to four exponential functions to describe the time dependent change of the relative amplitudes $A(t)$ of the T_2 range IV (T_2 > 300ms), which represented the intrusion of water into the peat matrix, and to calculate the time constants of the rate-limiting processes of peat swelling. The best re-

sults (large R^2, small standard errors and good reproducibility between replicates) were determined using a sum of three exponentials

$$A(t) = \sum_{i=3} A_i \exp\left(\frac{-t}{\tau_i}\right) + A_\infty. \quad (6)$$

A_i $(i = 3)$ is the relative amplitude of each exponential function, A_∞ the relative amplitude for infinite hydration time, t the hydration time [d], $\tau_{i\ (i=3)}$ the time constant of each first order process [d]. The reciprocal, $\frac{1}{\tau_i}$ $_{(i=3)}$, represents its rate constant, k, [d^{-1}].

According to the Arrhenius-Equation, the temperature dependency of the rate constant, k, of the water intrusion allows to calculate the activation energy, E_A, which is the minimum energy necessary for a specific process to occur [48]

$$\ln(k) = \ln(A^*) - \frac{E_A}{R}\left(\frac{1}{T}\right). \quad (7)$$

A^* is the pre-exponential factor (commonly written as A, but changed to A^* to avoid confusion with A used for relative amplitude), R the universal gas constant ($R = 8.314472$ J mol^{-1} K^{-1}), T the absolute temperature (K). The apparent activation energy gives information about the nature of the rate-limiting step of the investigated process. Chemical reactions are characterised by E_A > 60 kJ mol^{-1}, while physically controlled processes require E_A < 40 kJ mol^{-1} [49].

RESULTS AND DISCUSSION

Changes of Relaxation Time Distributions During Hydration

The T_1 and T_2 distributions of water protons in the two rewetted peat samples at the beginning and end of the swelling experiment are shown in Fig. (**1**) for peat 1 and Figure 2 for peat 2 for the temperatures 5°C (B+D) and 30°C (A+C). All relaxation time distributions consist of several peaks (up to five peaks for peat 2), which are in some cases hardly distinguishable. However, the relaxation time distributions in Figs. (**1** and **2**) show three features. Firstly, the shapes of the T_1 and T_2 distributions at the end of the hydration period are different to those directly after water addition (referred to as start in the Figures). The relative amplitudes at smaller T_1 and T_2 values increased and those at larger T_1 and T_2 values decreased for both peat samples. Parallel to this, the T_2 values of the peak maxima increased for peaks at smaller T_2

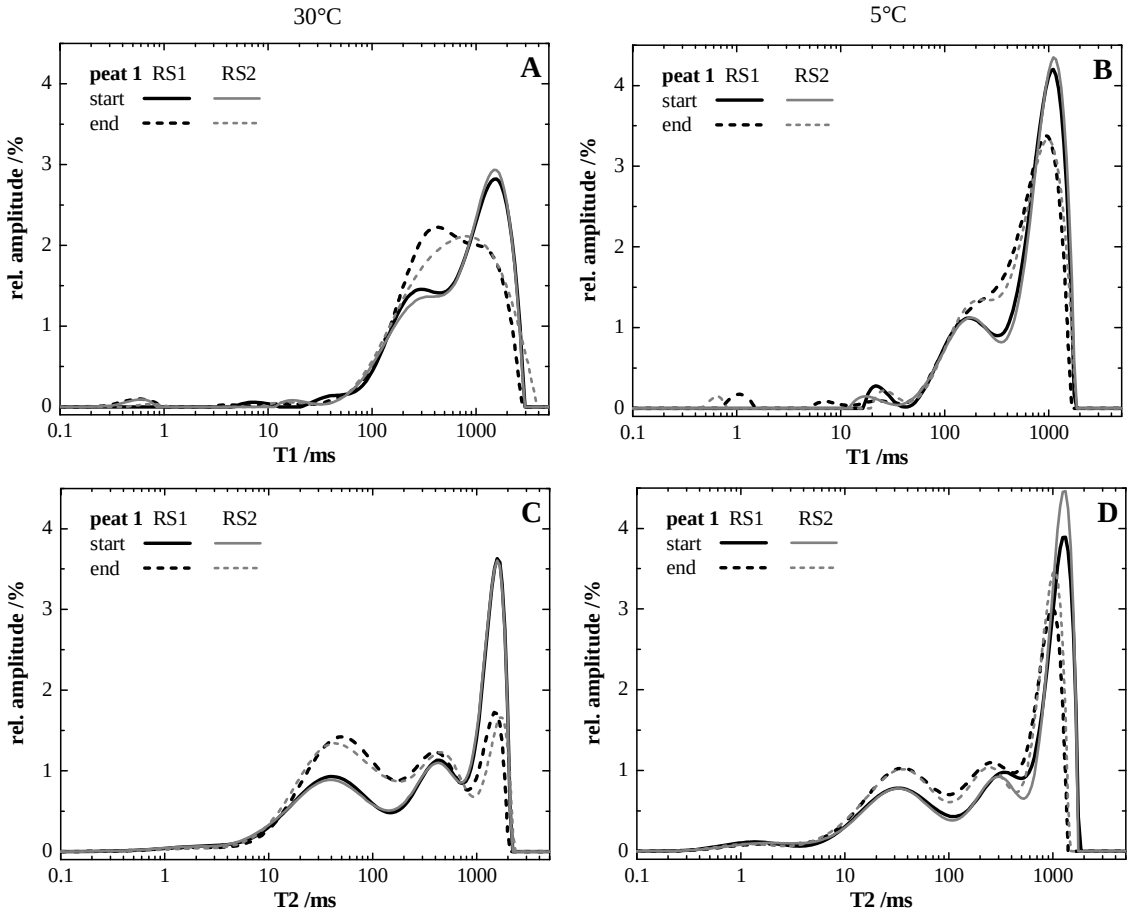

Fig. (1). T_1 and T_2 distributions of water protons in the rewetted peat 1 samples at the beginning and end of the swelling experiment determined at 5°C (**B+D**) and 30°C (**A+C**). The results of the two repetition samples or replicates (RS1 and RS2) are displayed.

(< 20 - 200 ms) and decreased for peaks at larger T_2 (> 200 ms). Secondly, the shapes of the T_1 distributions differ from the shapes of the T_2 distributions. Thirdly, the width of the T_1 and T_2 distributions for peat 2 are found to be broader than those of peat 1. Furthermore, the relative amplitudes at T_1 < 100 ms and at T_2 < 10 ms are larger for peat 2.

The sample weights and the total sum of amplitudes ($SI_{t=0}$) during hydration time of 5 to 7 months was constant within ± 2 % for all peat samples. After calibration with pure water at the different temperatures, $SI_{t=0}$ was used to calculate the NMR detectable amounts of water in the peat samples, which were comparable to those determined by gravimetric measurements. Hence, all water inside the peat samples was determined by the ^1H NMR relaxometry measurements and no water was lost during the long hydration times. In the course of hydration, the peat sample volumes increased and the calculated *Q* values were 1.5 for peat 1 and 2.0 for peat 2.

The relaxation time distributions of water in the two repetition samples of each peat (referred to as RS 1 and RS 2 in Figs. (**1** and **2**) were similar with each other for all hydration time points. The only exception was the T_1 distribution for the second repetition sample of peat 2 at 30°C (RS 2 in Fig. **2A**), which was not comparable to the one for RS 1 (Fig. **2C**).

Figs. (**1** and **2**) also show that the relaxation time distributions were affected by the incubation temperature. An increase of the peak relaxation times and of peak widths at higher temperatures was found. Eq. 7 was used to calculate the activation energies, E_A, of the peak relaxation time increase at the beginning and end of hydration time using $T_2^{-1} = k$. E_A was 4 - 12 kJ mol^{-1} for peat 1 and 3 - 16 kJ mol^{-1} for peat 2. T_2 of pure water increased from 1.5 s at 5°C to 2.8 s at 30°C and E_A of this T_2 increase was 16.3 ± 0.4 kJ mol^{-1}. Thus, the activation energies for the peat samples were smaller then or comparable to E_A of pure water. This suggests that the temperature dependency of the relaxation time distribution of water in the peat samples can be attributed mainly to increasing water diffusivity. Furthermore, the positive relation between peak relaxation time and temperature suggests that the proton relaxation in the peat samples was surface limited [50].

The large *Q* values indicated volumetric swelling [1] of both peats, but to a larger extent for peat 2. The decrease of the T_2 values for peaks at larger T_2 (> 200 ms) is consistent with the findings reported elsewhere and suggests swelling of peat [6, 12, 13]. The increase of the T_2 values of the peak maxima for peaks at smaller T_2 (< 20 - 200 ms) is contrary to Jaeger *et al.* [13] and Todoruk *et al.* [6]. However, a qualitatively comparable peak maxima shifting was also observed during the swelling of starchy sago beads (data not shown). The differences between the two repetitions of peat 2 at 30°C

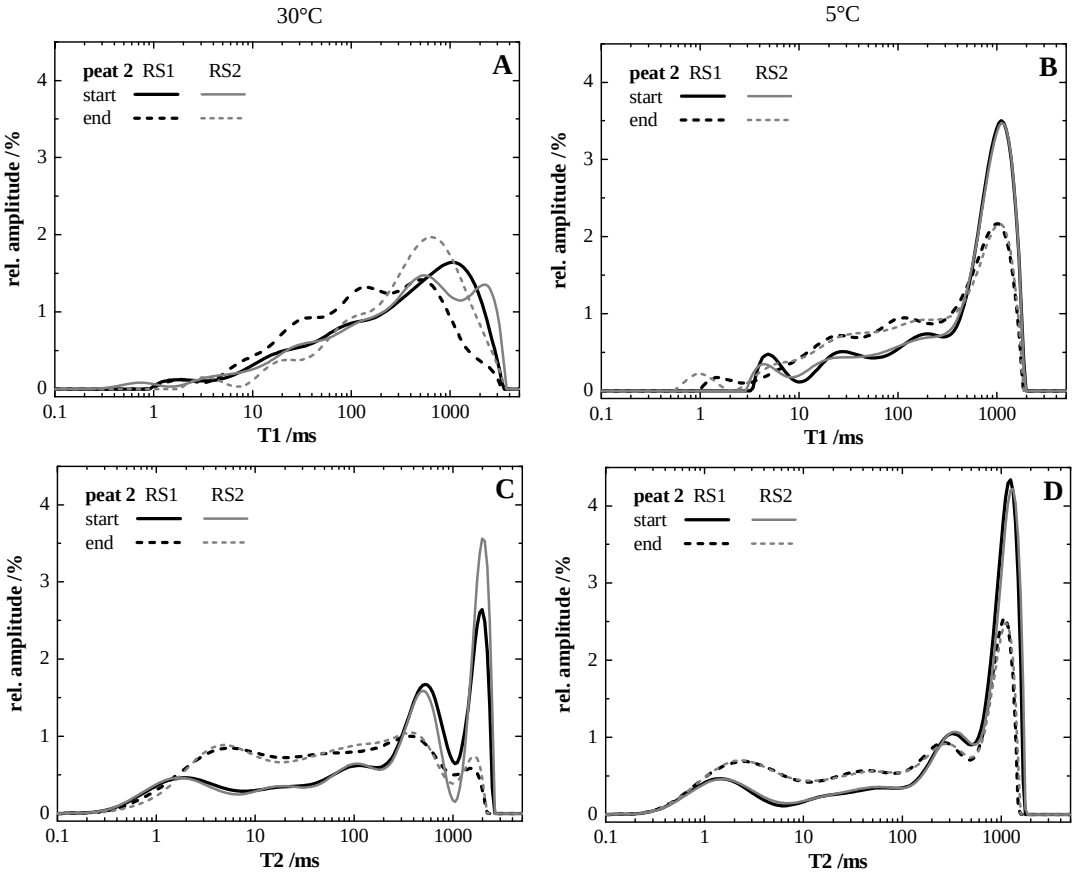

Fig. (2). T_1 and T_2 distributions of water protons in the rewetted peat 2 samples at the beginning and end of the swelling experiment determined at 5°C (**B+D**) and 30°C (**A+C**). The results of the two repetition samples or replicates (RS1 and RS2) are displayed.

may be due to the two weeks longer hydration time of RS 2 and resulting stronger peat swelling, which may have affected T_1 differently in the second repetition than in the first.

Water Distribution Versus Centrifugation Speed

The distribution of water in the two peat samples at the beginning, after 2 days and at the end of hydration time are represented as a function of centrifugation speed in Fig. (**3**). Direct after water addition (start), centrifugation at 500 RPM resulted in a dramatic decrease of the relative water contents of the peats to about 40 % of the original water contents. No significant changes of the relative water contents were observed for the next one to two centrifugation speeds (peat 1 and peat 2, respectively). For centrifugation speeds faster than 800 RPM (peat 1) or 1000 RPM (peat 2), the water contents decreased with increasing centrifugation speed, with an end point of ~15 % and ~25 % at 4000 RPM (peat 1 and peat 2, respectively). With increasing hydration time of the peat samples, the relative water contents at all centrifugation speeds increased. This observation was more pronounced for smaller centrifugation speeds, where the relative water contents at the end of hydration were almost two times larger than at the beginning. The water contents after two days of hydration for smaller centrifugation speeds were found to be between the values determined at the beginning and the end of hydration. For larger centrifugation speeds, they were comparable to the initial values. The observed changes were more pronounced for peat 2 than for peat 1.

The water distribution of RS 2 of peat 2 at the end of hydration (Fig. **3B**) was comparable to the one of RS 1 only for centrifugation speeds faster 2000 RPM. For centrifugation speeds slower 2000 RPM, the values of the relative water content were significantly larger. For the other peat samples, the two repetition samples were similar (day 2 was studied without any repetition sample).

With the assumption that every centrifugation speed represents a certain pore size and the represented pore size decreases with increasing centrifugation speed [51], it can be concluded that the pore size distribution changed significantly during peat hydration. This change was slow and takes place in two phases. The first phase started very soon after water addition and lasted for more than two days. It was characterised by the decrease of the number of very large pores (> 50 μm) represented by centrifugation speeds of 500RPM and the evolution of medium-sized pores 50 - 10 μm [51], represented by centrifugation speeds of up to 1000 RPM. The second phase started anytime after the first two days of hydration and resulted in the ongoing evolution of medium-sized pores 50 - 10 μm as well as of small-sized pores 10 - 1 μm [51], represented by centrifugation speeds of 1000 - 4000 RPM.

Fig. (**4**) shows the T_1 and T_2 relaxation times of water in the desaturated peat samples as a function of centrifugation speed (the same samples as presented in Fig. (**3**) without the sample of day 2) to test whether the observed changes of the relaxation time distributions in Figs. (**1** and **2**) were caused by surface relaxivity changes of the peat samples during hydration. The T_1 and T_2 relaxation times decreased with increasing centrifugation speeds, but were comparable for the beginning and for the end of hydration.

Again, the only exception was the sample 2 of peat 2 (Fig. **4B+D**) for which T_1 values were always larger than those of RS 1. In contrast, T_2 of RS 2 was larger only for centrifugation speeds slower than 2500 RPM, but comparable to those of RS 1 for larger centrifugation speeds. This implies that both the transverse and the longitudinal surface relaxivity decreased in RS 2 of peat 2. However, Fig. (**2A+C**) show that only T_1 but not T_2 distributions are different for the two repetition samples of peat 2 at 30°C. It, therefore, is more likely that the two repetitions were different in some physical properties which affected the dewatering by centrifugation. For instance, reduced water conductivity due to stronger water binding of entrapped water in a gel phase may result in a less effective dewatering by centrifugation, because smaller speeds cannot overcome the stronger water holding. It was found that at high centrifugation speeds faster 2000 RPM only the T_1 but not the T_2 and the relative water content values of the two repetition samples of peat 2 were different. Hence, it can be suggested that only the longitudinal, but not the transverse surface relaxivity of RS 2 of peat 2 at 30°C increased during hydration. This may be due to a stronger decrease of the water mobility in the vicinity of the peat surface.

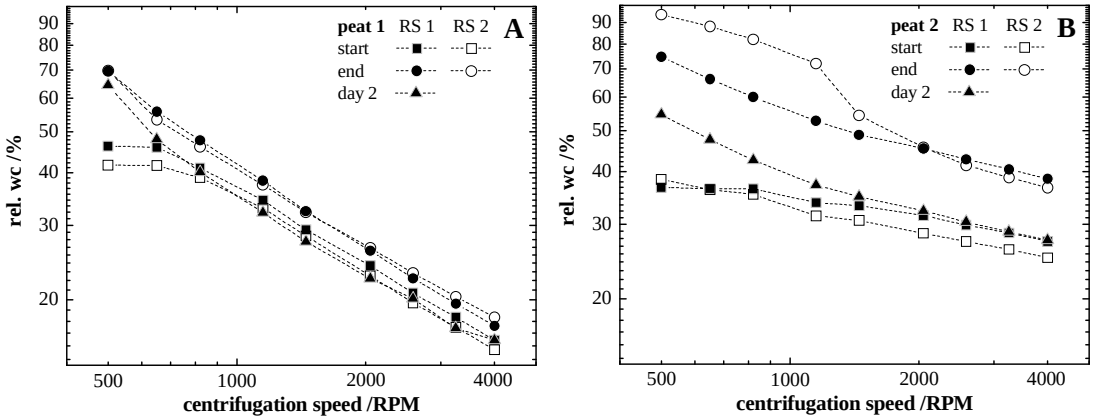

Fig. (3). Distributions of water in the two peat samples at the beginning, after 2 days and at the end of hydration time (the 30°C samples at the end of hydration measured at 19°C) as a function of centrifugation speed. The results of the two repetition samples or replicates (RS1 and RS2) are displayed (not for day 2).

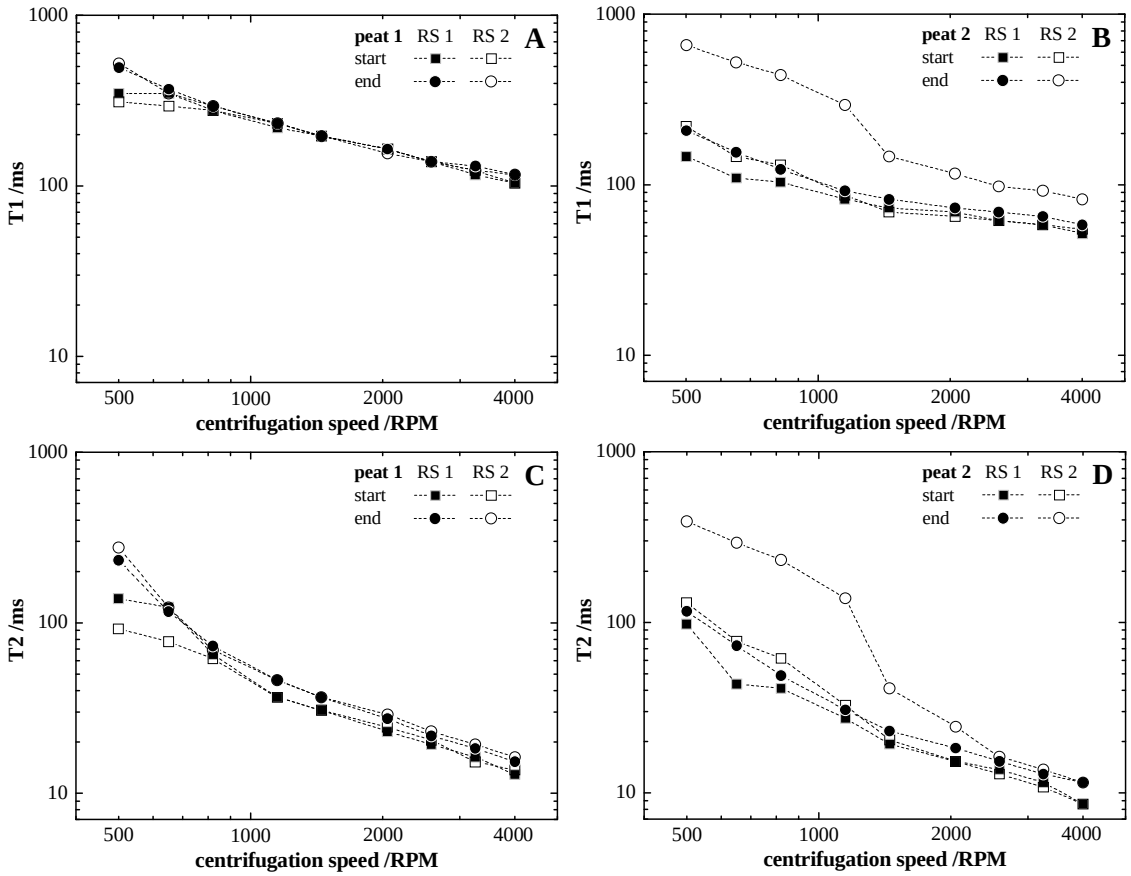

Fig. (4). T_1 and T_2 relaxation times of water in the two desaturated peat samples as a function of centrifugation speed (the same samples as presented in Figure 3 without sample of day 2). The results of the two repetition samples or replicates (RS1 and RS2) are displayed.

For peat 1, the T_1 and T_2 values at 500 RPM were smaller at the beginning than at the end of hydration (Fig. **4A+C**). The relative water content at the beginning of hydration was constant between 500 RPM and 650 RPM (Fig. **3**). Thus, the smaller T_1 and T_2 values were due to only pores smaller than represented by centrifugation speeds of 500 - 650 RPM were existent in the desaturated samples direct after water addition. With the exception of RS 2 of peat 2 at 30°C, the longitudinal and the transverse surface relaxivities of the two peat samples did not change significantly during hydration time. Surface relaxivity changes may be only to some extent responsible for the observed changes of the T_1 distributions, but not for those of the T_2 distributions in the course of hydration of the two peats soil samples.

Calculation of Time Constants and of Apparent Activation Energy

Fig. (**5**) shows the changes of relative amplitudes of the four T_2 ranges (I: 0.1 - 3 ms; II: 3 - 30 ms; III: 30 - 300 ms and IV: > 300 ms) in the T_2 distribution of water in the two rewetted peat soil samples at 30°C (Fig. **5A+C**) and 5°C (Fig. **5B+D**) as a function of hydration time. Within the first hours after water addition, the relative amplitudes for T_2 > 300 ms decreased very fast followed by an ongoing slower decrease, which lasted for several months. This slow decrease was not fully completed until the end of the available experiment time of 5 to 7 months. Parallel to this decrease the relative amplitudes of the T_2 ranges II and III increased during the course of hydration. For peat 1 mainly the amplitudes of the T_2 range III (30 - 300 ms) increased. For peat 2 the amplitudes of the T_2 range II (3 - 30 ms) increased. Similar to the decrease of the relative amplitudes for T_2 > 300 ms, the increases of amplitudes at smaller T_2 were very fast in the beginning and much slower after a few days lasting until the end of the experiment.

From the contact angle experiment it can be concluded that the peat surfaces were fully wettable after water addition, because the water drop needed for the contact angle measurement did not rest at the peat surface, but was sucked into the matrix immediately. The T_{1B} and T_{2B} bulk relaxation times in the extracted peat soil solutions measured at 19°C were with 2.0 ± 0.3 s comparable to that of pure water $T_{1,2B}$ = 2.3 s and did not change significantly during the course of hydration for any of the two peats. Thus, the time dependent changes of the relative amplitudes of the T_2 ranges represented mainly the intrusion of water into the peat matrix or water re-distribution, but not surface wettability changes or changes of the bulk relaxation times.

For both peats, three time constants in the range of minutes (fast), hours (medium fast) and several weeks to months (slow) for the rate-limiting processes of water intrusion (decease of the relative amplitudes for T_2 > 300 ms) were calculated with Eq. 6 (Table **2**). The time constants of the three processes were slightly larger for peat 1 and the relative amounts of re-distributed water smaller than for peat 2. In

total, about 20 % (peat 1) and 30 - 40 % (peat 2) of the total water in the peat samples took part in the water intrusion. All time constants decreased with increasing temperature, which allowed the calculation of apparent activation energies, E_A, of the three rate-limiting processes of water intrusion using Eq. 7. The activation energies (Table **2**) were comparable for the two peat samples and ranged between 5 kJ mol^{-1} (fast process), 15 - 25 kJ mol^{-1} (medium fast process) and 40 - 50 kJ mol^{-1} (slow process). Thus, E_A of the medium fast process is comparable to the value determine for pure water (see above), whereas it is smaller for the fast, but larger for the slow process.

The amounts of re-distributed water during hydration of the peats were comparable to those found in mineral soil samples [13]. The water re-distribution was accompanied by a reduction of T_2 for 20 - 40 % of the total water, indicating a decrease in mobility of the involved water molecules during hydration [52]. The fast process of water re-distribution was not observed in soil samples until now, which may be due to the faster water addition of two instead of 15 minutes compared to similar studies [12], the faster measurement of T_2 compared to T_1 [2] and the better time resolution within the first minutes after water addition with one T_2 measurement every five minutes compared to one measurement per day [2, 12, 13] or every 30 minutes [6]. The medium fast process was also observed in other studies [6, 12, 13]. The time constant of the slow process is up to 10 to 15 times larger than reported elsewhere [2, 6, 12, 13]. The apparent activation energies of the three processes are in the lower range as reported by Todoruk *et al.* [6] or even smaller. As they [6] found a negative relation between SOM content and the value of the apparent activation energy, this may be due to the high organic matter contents of about 99 % of the two peats in this study. However, it cannot be excluded that dissolution of paramagnetic substances may have additionally increased the values of the apparent activation energy in their study, because the contribution of the soil solution to the proton relaxation was not considered. It was shown in a previous study [19] that the concentration of iron and manganese in the solution of peat is generally smaller than in the solution of mineral soil samples and that the iron and manganese concentration in soil solution may increase during hydration.

The apparent activation energies calculated for the fast process are comparable to the energy of 6.3 kJ mol^{-1} required to just break the hydrogen bond in a locally symmetric, strongly H-bonded domain in water [53] leaving the molecules essentially in the same position. E_A of the medium fast process is comparable to the value reported for water self-diffusion [25], and indicates diffusion processes of water.

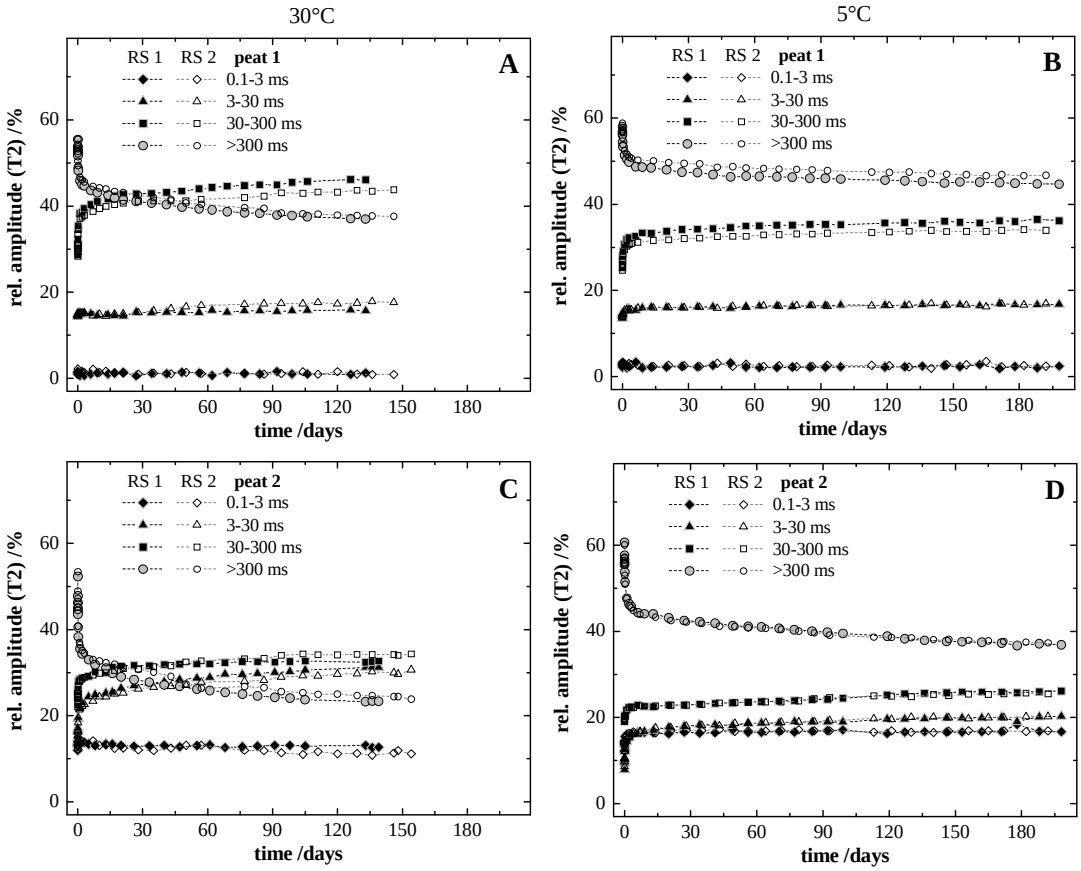

Fig. (5). Changes of the relative amplitudes of the four T_2 ranges (I: 0.1 - 3 ms; II: 3 - 30 ms; III: 30 - 300 ms and IV: > 300 ms) in the T_2 distribution of water in the two rewetted peat soil samples at 30°C (Fig. **5A+C**) and 5°C (Fig. **5B+D**) as a function of hydration time. The results of the two repetition samples or replicates (RS1 and RS2) are displayed.

Table 2. Results of the Peat Swelling Kinetics (i.e. Decrease of the Relative Amplitude of T2 > 300 ms) and Apparent Activation Energies (E_A) of the Three Determined Processes Governing the Swelling of peat. *SE* Standard Error

Sample	Process	Time Constant (30°C to 5°C)	rel. Amount of Total Water/%	$E_A \pm SE$/kJ mol^{-1}
peat 1	fast	25-35 min	5-7	6 ± 3
	medium fast	20-50 h	~5	24 ± 4
	slow	55-330 d	7-9	49 ± 7
peat 2	fast	15-20 min	10-17	4 ± 2
	medium fast	20-30 h	7-9	16 ± 6
	slow	45-210 d	11-16	42 ± 5

The larger activation energies of the slow process suggest physical or physicochemical controlled processes, such as water diffusion or reorientation of SOM chains during hydration [6, 38, 49].

T_1 - T_2 and T_2 - D Two-Dimensional NMR Measurements

The results of the T_1 - T_2 and T_2 - D two-dimensional NMR measurements of the two peats at the beginning and end of hydration time at 30 MHz and 20°C are shown in Fig. (**6**). Direct after water addition, most of the water protons relaxed with T_1 and T_2 relaxation times comparable to pure water, which is represented by the high intensity areas close to the 1:1 line (white line) in Fig. (**6A**) for peat 1 and Fig. (**6D**) for peat 2. However, some water protons at shorter relaxation times relaxed at smaller T_2 than T_1 values. This is represented by the deviation of the intensity areas from the 1:1 line. This deviation was more pronounced at the end of the hydration time (Fig. **6B+E**), where the amount of water protons relaxing at smaller relaxation times was increased (Figs. **1**, **2** and **5**). Whereas the deviation from the 1:1 line appeared to be continuously for peat 1 (Fig. **6B**), it was more step-wise for peat 2 (Fig. **6E**). As a result of this deviation, the T_2 values were about ten times smaller than the T_1 values at small relaxation times. Furthermore, both figures show that each T_1 is related to one T_2 value and vice versa. Thus, each T_1 population was related to one T_2 population in the T_1 and T_2 distributions in Figs. (**1** and **2**), which allows a quantitative comparison of the T_1/T_2 ratios of water in the peat samples used in the swelling kinetics experiment (see next section).

The T_2 - D correlation spectra of water in the two peat samples (RS 1 only) at the end of hydration at 20°C are shown in Fig. (**6C**) (peat 1) and Fig. (**6F**) (peat 2). For larger relaxation times (T_2 > 30 ms), the apparent diffusion coefficient of water in the two peat samples was comparable to the one of free water with D_{app} = 2.03 x 10^{-9} m^2 s^{-1} [54]. For smaller relaxation times (T_2 < 30 ms), the apparent diffusion coefficient of water was reduced to D_{app} = 1.2 x 10^{-9} m^2 s^{-1} for peat 1 and D_{app} = 0.7 x 10^{-9} m^2 s^{-1} for peat 2. Thus, the translational mobility of 22 % (peat 1) and 35 % (peat 2) of the total water was reduced compared to that of free water. At the beginning of hydration (data not shown), it was found that the translational mobility of only 16 % (peat 1) and 12 % (peat 2) of the total water was reduced. This indicates that the translational mobility of 6 % and 23 % of the total water in peat 1 and peat 2 was reduced during hydration, respectively. The reduced translational water mobility in the peats may be due to the larger surface to volume ratios of smaller pores [55] or due to water entrapment inside a gel phase, where the water mobility is affected by the polymer chains, as shown for e.g. agar gels [56].

The T_1 - T_2 correlation spectra of the two peats were very different from those of sedimentary rock samples [42]. The main difference is the stronger deviation of the high intensity area from the 1:1 line for the peats. To compare this phenomenon found in peat with other materials that are able to swell and form gel phases, we studied additionally different reference materials like agar, starch (1 - 2 mm sago beads) and allophane gel (1.25 SiO_2 * Al_2O_3 * 3.2 H_2O). For agar gel (c = 30 g L^{-1}), the T_1 - T_2 correlation spectrum showed one high intensity area in the shape of a circle at T_1 = 2000 ms and T_2 = 41 ms (data not shown). The resulting T_1/T_2 ratio was about 50 at 30 MHz. Fig. (**7A**) shows that the T_1/T_2 ratios of water in agar gels at 7.5 MHz strongly increase as a function of the agar concentration. The T_1/T_2 ratio in the agar gel with c = 30 g L^{-1} was with 27 smaller than at 30 MHz, because T_1 was with 1240 ms much smaller than at 30 MHz (T_1 = 2000 ms). T_2 was with 45 ms at 7.5 MHz comparable to the value at higher field strength (T_2 = 41 ms). For inorganic allophane gel (wc = 5.5 ± 0.5 g g^{-1}), the T_1 - T_2 correlation spectrum was qualitatively comparable to the one of the agar gel, but with smaller relaxation time values of T_1 = 330 ms and T_2 = 10 ms (data not shown). The calculated T_1/T_2 ratio was 33 at 30 MHz and 25 at 7.5 MHz, because T_1 was smaller at 7.5 MHz and T_2 similar to that at higher field strength.

Fig. (**7**) also represents the T_1 - T_2 (Fig. **7B**) and the T_2 - D (Fig. **7C**) correlation spectrum of water in swollen sago beads. Sago is a starch extracted from the pith of sago palm stems (*Metroxylon sagu*) and is commonly used in the food industry. In contrast to agar and allophane gel, the T_1 - T_2 spectrum of swollen sago beads consist of a broad distribution, which is more similar to the one determined for peat 1 at the end of hydration. However, the deviation of the high intensity area from the 1:1 line is stronger and the calculated maximal T_1/T_2 ratios are with 30 - 40 comparable to those of the agar and allophane gels. The T_2 - D spectrum shows that for some water at smaller T_2 the water mobility was with D_{app} = (0.5 - 1.8) x 10^{-9} m^2 s^{-1} smaller than for free pure wa-

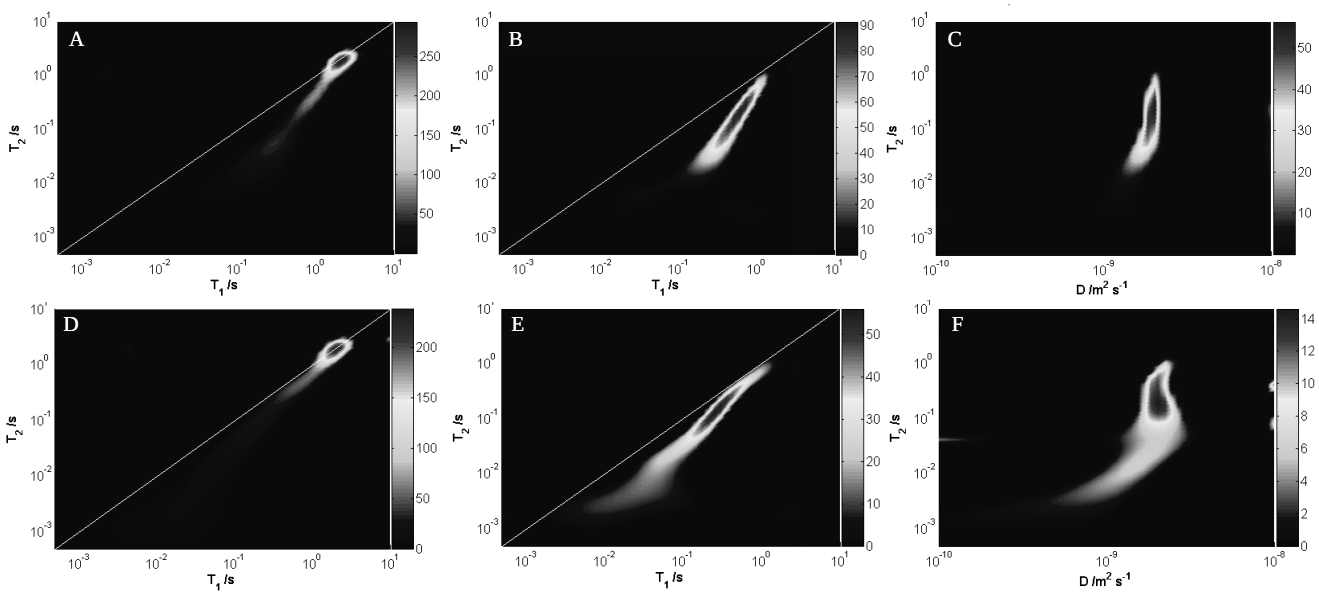

Fig. (6). Two-dimensional T_1 - T_2 - and T_2 - D - correlation spectra of water in peat 1 (**A-C**) and peat 2 (**D-F**) at the beginning (**A+D**) and end of hydration time (**B+E** and C+**F**) at 30 MHz determined at 20°C.

ter, which is comparable to peat 2 at the end of hydration. Thus, the two-dimensional correlation spectra of the two peats were qualitatively comparable to those of the swollen sago beads suggesting similar properties in terms of proton relaxation and water mobility.

For all peat samples and reference materials, T_2 was determined as a function of echo time to estimate the contribution of T_{2D} to the total proton relaxation. The T_2 distribution did not change significantly with increasing echo times for all samples. Furthermore, T_{2D} was in the range of seconds. Thus, the contribution of T_{2D} to the total proton relaxation was negligible for all studied peat and reference samples. Consequently, the calculated large T_1/T_2 ratios of water in these samples were not due to diffusion in internal magnetic field gradients, which had to be very small in all studied peat and reference samples.

The findings for water in agar, allophane gels and swollen sago suggest longer correlation times for the dipole interactions of the bound water protons compared to free water [25] due to water structuring [17, 23]. Thus, swelling of these materials reduced both the rotational and translational water mobility compared to free water, which is consistent with the findings for wheat starch pastes [23].

Water State Characterization by ^{1}H NMR Relaxometry and DSC

T_1/T_2 Ratios as a Measure of the Water State in Peat Samples

Fig. (**8**) shows the T_1/T_2 ratios of the rewetted peat soil samples at the beginning (19°C) and end of hydration time (swollen at 30°C, ratios determined at 19°C) as a function of the relative water content (rel. wc). The rewetted peat samples were measured in a fully water saturated (black) and in a step-wise desaturated state (grey) after centrifugation (i.e. the original peat samples from the swelling kinetics experiment at 30°C shown in Fig. **4**). The calculation of the T_1/T_2 ratio started from 7.5 % rel. wc instead of 0 %, because the number and position of the peaks at very small T_1 values (Fig. **1A+B**, T_1 < 20 ms; Fig. **2A+B**, T_1 < 2 ms) were not reproducible for the repetition samples.

The T_1/T_2 ratios calculated from the step-wise desaturated peat samples were comparable to those from the relaxa-

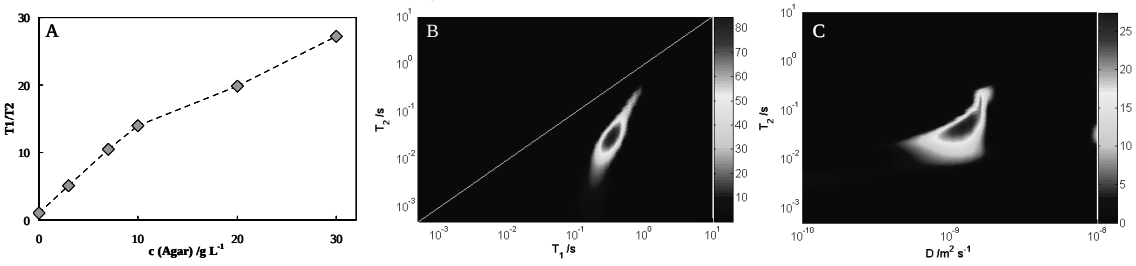

Fig. (7). T1/T2-ratio of water in agar gels as a function of the agar concentration at 7.5 MHz (**A**) and two-dimensional T_1 - T_2 - (**B**) and T_2 - D - correlation spectra of water swollen starchy sago beads (**C**) at 30 MHz determined at 20°C.

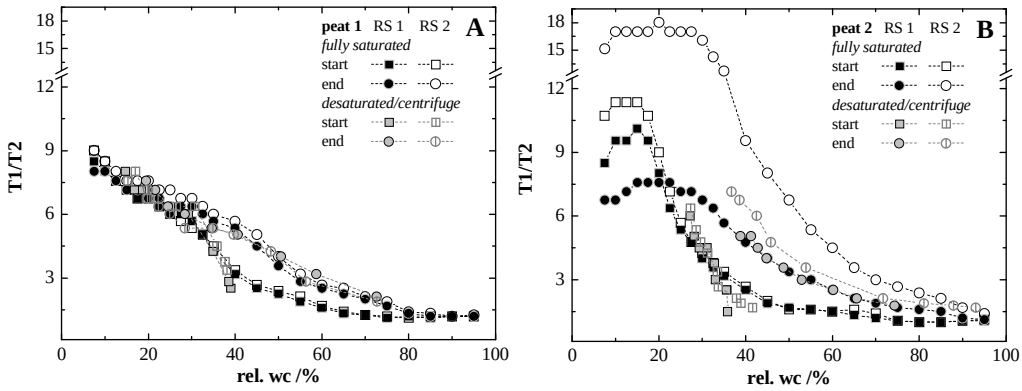

Fig. (8). T1/T2 ratios of the rewetted peat soil samples at the beginning (start) and end of hydration time as a function of the relative water content (rel. wc) determined from the relaxation time distributions at 19°C. The T1/T2 ratios at the end of hydration were calculated from the 30°C samples measured at 19°C. The rewetted peat samples were measured in a fully water saturated and step-wise desaturated (centrifugation) state. Relative water contents were calculated with Eq. 4 (saturated samples) and Eq. 5 (desatureated samples). The results of the two repetition samples or replicates (RS1 and RS2) are displayed.

tion time distributions of the fully water saturated peat samples at the beginning and end of hydration (Fig. **8**). The only exception was again RS 2 of peat 2 where the T_1/T_2 ratios of the desaturated sample were smaller than those of the fully saturated one. This was maybe due to the decanting of the peat samples into the centrifugation tube and the resulting air contact and re-packing of the sample. The T_1/T_2 ratios of water in the peat samples increased with decreasing rel. wc from 1.1 (at rel. wc = 100 %) to 8 - 9 (peat 1) and 6 - 18 (peat 2) at rel. wc of 10 - 20 %. The amount of water with T_1/T_2 ratios larger 3 increased from 40 % at the beginning to about 60 % (or 80 % for RS 2 of peat 2) at the end of hydration. The large T_1/T_2 ratios of RS 2 than RS 1 of peat 2 were mainly due to the different T_1 distribution (see Fig. **2A**).

It was found for both peat samples that at the beginning (not shown) and end (Fig. **9**) of hydration the amount of water with T_1/T_2 ratios larger 3 increased with increasing temperature. Furthermore, the T_1/T_2 ratios between 30 % and 80 % rel. wc were always larger at 30°C than at 5°C (Fig. **9**). Eq. 7 was applied to calculate the activation energies, E_A, of the temperature dependent increase of the observed T_1/T_2 ratio increase by using $T_1/T_2 = k$. The calculated E_A at the beginning and end of hydration was 3 - 12 kJ mol^{-1} for both peat samples. It, therefore, can be suggested that the temperature dependency of the T_1/T_2 ratios of water in the peat samples can be attributed mainly to increasing water mobility (diffusion and rotation) at higher temperatures. Consequently, at least three types of water can be distinguished by the different T_1/T_2 ratios. Type 1 is represented by small relaxation times and large T_1/T_2 ratios (> 6 at rel. wc smaller 30-40 % in Fig. **9**). Type 3 is represented by long relaxation times and small T_1/T_2 ratios between 1.0 and 1.5. Type 2 can be considered as the transition from type 1 to type 3 and its amount of water is depending on the mobility of water (see Fig. **9**). We suggest that water type 1 represents bound or structured water, type 2 exchange water and type 3 bulk-like free water.

Some of the water in the peat samples was found to be similar to free pure water over the whole period of hydration (T_1/T_2 ratio ~ 1). Another part of the water changed its state after addition to the peat sample as represented by larger T_1/T_2 ratios, which were much larger than generally found in rock core samples [24]. These large T_1/T_2 ratios of water in peat were in the same range as determined for agar gel or swollen sago beads (Fig. **7**). This suggests that this water was structured by the peat in a comparable way as reported for water in starch [17]. Consequently, the large T_1/T_2 ratios in the peat samples may be due to a water structuring in the vicinity of the peat surfaces and the resulting longer rotational correlation times of the water molecules within this water phase [17]. The amount of structured water increased during hydration, because the amount of water with T_1/T_2 ratios larger 3 increased by a factor of 1.5. This indicates that about 20 % of the total water significantly changed its state during the swelling, which suggests that the amount of water within a gel phase in the peats increased.

Cryo-NMR Relaxometry: Determination of Non-Freezable and Loosely Bound Water

The amounts of non-freezable water at -34°C of the two peat samples determined by Cryo-NMR ranged between 0.43 g g^{-1} d.m. and 0.55 g g^{-1} d.m. and increased by 5 % (peat 1) and 20 % (peat 2) during hydration (Table **3**). From the freezing behaviour determined by DSC, it can be concluded that this water was not frozen until -90°C (data not shown). The amounts of loosely bound water at -5°C were about 5 to 10 times smaller than those of the non-freezable water at -34°C and increased only for peat 2 during hydration (Table **3**). However, the amount of loosely bound water in peat 2 was 20 % to 50 % smaller than for peat 1.

The relaxation time of water in the air dried peat samples measured at 19°C, where only non-freezable water existed, was 293 ± 3 µs for peat 1 and 267 ± 3 µs for peat 2. The T_2 values determined by Cryo-NMR represent the relaxation times of non-freezable water and of loosely bound water in the frozen peat samples at the maximal water holding capacity. Table **3** shows that the T_2 values for each peat increased in the following order: non-freezable water in air dried peat, non-freezable water at -34°C and loosely bound water in the

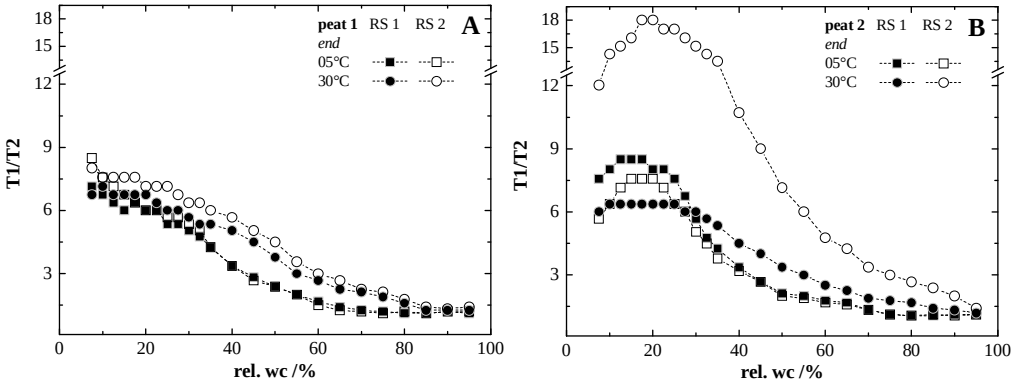

Fig. (9). T1/T2 ratios of the rewetted peat soil samples at the end of hydration time as a function of the relative water content (rel. wc) determined from the relaxation time distributions of water in the fully saturated peat samples at 5°C and 30°C. The results of the two repetition samples or replicates (RS1 and RS2) are displayed.

frozen peat samples. Furthermore, additionally to the increasing amounts of non-freezable water at -34°C and of loosely bound water the T_2 values of both water types increased during hydration.

The amounts of non-freezable water were comparable to those reported for different starch materials [15] or peats [7], but were larger than those reported by Schaumann *et al.* [14]. Increasing amounts of non-freezable water during hydration were also found for starch gels [52]. The relaxation times of the two types of bound water were about one order of magnitude larger than determined for peat at 300 MHz [7]. The differences, therefore, may be due to the 10 times higher magnetic field strengths compared to this study.

DSC: Determination of Different Water States and of Melting Enthalpy of Freezable Water in Peat

The DSC thermograms in Fig. (**10**) show the endothermic melting peaks of free pure water and soil solutions of the two peat samples extracted at the end of hydration (Fig. **10A+B**). Furthermore, they show the melting peaks of the freezable water in the fully saturated (Fig. **10C+D**) and in the desaturated peat samples after centrifugation at 4000 RPM (Fig. **10E+F**) at the beginning and end of hydration time. The number of melting peaks of water in the fully saturated peat samples increased from one at the beginning (broad peak around +2°C in Fig. **10C+D**) to two peaks at the end of hydration (one sharp peak around 0°C and one broad peak between +2°C and +5°C). For the desaturated samples, a clear splitting of the melting peak into one sharp and one broad peak was observable at the beginning as well as at the end of hydration (Fig. **10E+F**). In contrast to the fully saturated peat sample, the position of the sharp peak was around -1°C and the width of the broad peak was significantly smaller. The onset of the melting peak was between -5°C and -10°C for both peats. The DSC thermograms of free pure water and soil solutions consisted of only one melting peak with a very sharp onset at -3°C to -1°C and a maximum between +1°C and +2°C. For agar gel (30 g L^{-1}), the thermogram consisted of a sharp peak at -0.3°C and a broad peak at 5°C (not shown).

Fig. (**11**) shows that the peak temperature in the desaturated peat samples after centrifugation at 4000 RPM at the end of hydration time (Fig. **10E+F**), agar gel, water saturated sand 150 µm and free pure water increased with increasing

Table 3. Results of the Cryo-NMR and DSC Measurements of the Two Peats at the Beginning and End of Hydration Time. *SD* Standard Deviation, *SE* Standard Error, n.s. not Significant. T_2 of Water in the Air Dried Samples was 293 ± 3 µs for Peat 1 and 267 ± 3 µs for Peat 2. No Enthalpic Peak was Observed in the DSC Thermogram for Both Air Dried Peat Samples

Sample		Cryo-NMR				DSC			
		Non-Freezable Water at -34°C		Loosely Bound Water at -5°C		Non-Freezable Water	Melting Enthalpy of Water in Peat	Enthalpy Sharp Peak	Water Content Sharp Peak
		wc ± *SD* /g g^{-1} d.m.	T_2 ± *SD* /µs	wc ± *SD* /g g^{-1} d.m.	T_2 ± *SD* /µs	wc ± *SE* /g g^{-1} d.m.	ΔH_f ± *SD* /J g^{-1}	H_f ± *SD* /J g^{-1} d.m.	wc ± *SD* /g g^{-1} d.m.
peat 1	start	0.524 ± 0.001	435 ± 2	0.110 ± 0.001	925 ± 5	0.85 ± 0.11	366 ± 8	199 ± 38	0.54 ± 0.10
	end	0.553 ± 0.005	469 ± 5	0.106 ± 0.001	973 ± 26	0.77 ± 0.05	347 ± 7	265 ± 42	0.71 ± 0.11
peat 2	start	0.428 ± 0.007	402 ± 3	0.058 ± 0.001	794 ± 6	0.54 ± 0.24	329 ± 44	95 ± 11	0.28 ± 0.03
	end	0.522 ± 0.012	568 ± 83	0.083 ± 0.001	1047 ± 92	0.60 ± 0.08	326 ± 9	158 ± 26	0.49 ± 0.06

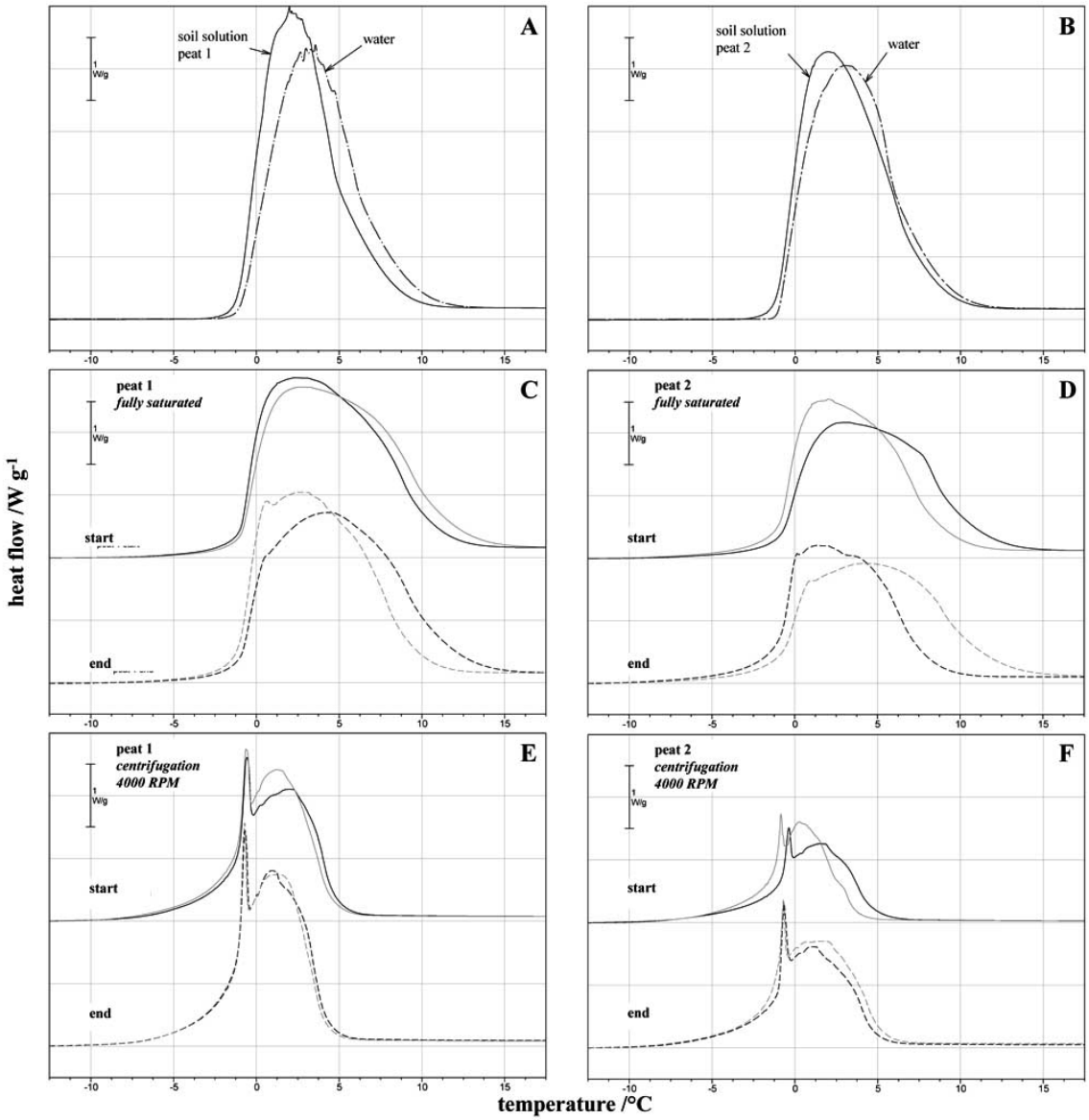

Fig. (10). DSC thermograms of free pure water and soil solutions of the two peat samples extracted at the end of hydration (**A+B**) and of the freezable water in the fully saturated (Fig. **10C+D**) and in the desaturated peat samples after centrifugation at 4000 RPM (Fig. **10E+F**) at the beginning and end of hydration time. The results of two of the three repetition samples used in the DSC are displayed as black and grey coloured curves.

heating rate. Thus, the melting of freezable water was kinetically controlled in all studied samples. However, the heating rate dependence was pronounced stronger for the broad peak than for the sharp peak. Furthermore, the heating rate dependence of the broad peak of the two peats was less pronounced than for agar gel, but stronger than for free pure water. For peat 1, it was comparable to sand 150 μm.

The amounts of non-freezing water determined from DSC were ~0.8 g g^{-1} for peat 1 and ~0.6 g g^{-1} for peat 2 and were comparable for the beginning and the end of hydration (Table **3**). The melting enthalpies of freezable water, ΔH_f, in the peats (Table **3**) were in the same range as those of free pure water and of soil solution 338 ± 8 J g^{-1} and decreased slightly only for peat 1 during hydration. To test whether the amount of water, represented by the sharp peak in the DSC thermogram, increased during hydration, the enthalpy of the sharp peak, H_f, (integral between peak onset at low temperature and minimum between the sharp and broad peak using the same baseline as for the total peak) was calculated for the peat sample after centrifugation at 4000 RPM. This made the observation of the sharp peak at the end of hydration possible for the full saturated peat samples. Assuming a melting enthalpy independent of the water binding state, we estimated the water content from $H_f / \Delta H_f$ (H_f per gram of dry peat), of the sharp peak for the beginning and end of hydration. Table **3** shows that this calculated water content, represented by the sharp peak, increased for both peat samples during hydration. However, this increase was significant only for peat 2, where the water content increased by about

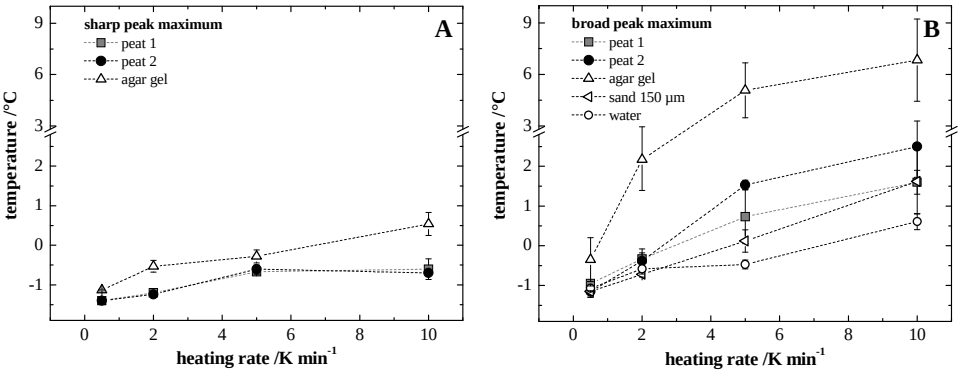

Fig. (11). Maxima of the DSC melting peaks of the desaturated peat samples after centrifugation at 4000 RPM at the end of hydration time (Fig. **10E+F**), agar gel (30 g L^{-1}), water saturated sand (particle size 150 µm) and free pure water as a function of heating rate.

60 %. This water accounts for 3 - 5 % of the total water in peat 1 and 6 - 11 % in peat 2.

A melting point depression was found for some water in the peats, which was not caused by dissolved salts in the soil solution. The melting characteristic of the water was strongly affected by the peat matrix and resulted in a splitting into (at least) two to three different types of water represented by the broad onset at low temperatures and the two peaks in the DSC thermograms, respectively. The broad shape of the onset may be due to the binding forces for water molecules within this boundary phase, which change strongly with increasing distance from the peat surfaces. At a certain distance from the surfaces and outside this boundary phase, the water molecules are still affected by the surfaces but in a more uniform way. These uniform conditions resulted in the formation of the sharp melting peak between -2°C and 0°C. We thus assume that the sharp peak mainly represents loosely bound water in peat. The shape of the broad melting peak of water in the fully saturated peat samples is different than for free pure water or for soil solution. However, the temperature range and maxima are comparable to water and soil solution where no loosely bound water exists (Fig. **10**). Hence, the broad melting peak may represent freezable bulk water, but additionally water that was still affected by the peat matrix.

According to the findings for maltodextrin gels [15], it can be suggested that the melting peak splitting of water in peat was due to the entrapment of water in a gel phase. By interpreting the energy transformation related with the sharp peak as quantitative measure for the amount of water in gels, the water contents related to the sharp peak at the beginning and end of hydration (Table **3**) indicated the formation of new and/or the change of existing gel phases during hydration. This would then indicate that the amount of water in gels increased during hydration and that some water was entrapped in gel phases shortly after water addition. This suggests an initial formation of gel phases in peat after surface wetting.

A splitting of the melting peak of water in peat in the DSC thermograms was also found by McBrierty *et al.* [7] and by Schaumann [14] for peats at water contents below the maximal water holding capacity. For peats with relatively high water contents, no splitting of the melting peak was observed [7]. The melting enthalpies of freezable water and the amounts of non-freezable water reported by McBrierty *et al.* [7] and Schaumann [14] were smaller than the values calculated in this study. The peak maxima are located at lower remperatures than reported by McBrierty *et al.* [7], but at higher temperatures than those reported by Schaumann [14]. In the first study, both peak maxima were detected above 0°C, whereas in the latter both peak maxima were found below 0°C. This may be due to the higher heating rates compared to our study or because different peat samples were used. Schaumann [14] found a heating rate dependence only for the broad peak and concluded that the broad peak represents loosely bound water and the sharp peak bulk-like water, which is contrary to the conclusions of this study. These differences may be due to the much higher degradation state and the lower water contents of 0.4 - 0.6 g g^{-1} of the peats used by Schaumann [14] and due to the different experimental setups (hydration from the gas phase, higher heating rates). For gelatine gels, Liu and Yao [57] attributed the sharp peak to loosely bound water (referred as "intermediate" water) and the broad peak to free water.

Comparison of the Results Determined by ^{1}H NMR and Cryo NMR Relaxometry and DSC

The amounts of non-freezable water determined by DSC were larger than those from Cryo-NMR, but were in the range of the sum of non-freezable and loosely bound water determined by Cryo-NMR (Table **3**). 3 - 5 % of the total water and 10 - 13 % were determined as non-freezable water in peat 1 and peat 2, respectively. The value for peat 2 agrees roughly with the beginning of the plateau at large T_1/T_2 ratios observed in Fig. (**8B**). For peat 1, no T_1/T_2 ratio was calculated at this low relative water content (see above). The sum of non-freezable water and water represented by the sharp peak in the DSC thermogram accounts for 8 - 10 % of the total water in peat 1. This value agrees with the largest T_1/T_2 ratio in Fig. (**8A**). In peat 2, this sum of the two water types accounts for 17 - 25 % of the total water, which agrees with the end of the plateau with large T_1/T_2 ratios in Fig. (**8B**). This suggests that the large T_1/T_2 ratios of water in the peat samples were related to non-freezable water and water represented by the sharp peak in the DSC thermograms (loosely bound water and water in gels). Thus, the observed

changes in the T_1/T_2 ratios during hydration may be due to the increasing of amounts of these two water types.

From the water state characterization by ^1H NMR and Cryo NMR relaxometry and DSC we conclude that a layered bound water phase existed inside the peats. This phase consisting of several layers of non-freezable and loosely bound water, whereas the binding forces and, consequently, the water structuring decreases with increasing distance from the peat surfaces resulting in higher mobility of the water molecules. This layered bound water phase includes water entrapped in gel phases. During swelling, the amounts of bound water as well as the mobility of the water molecules inside the bound water phase increased, which indicates a water intrusion into the peat matrix as well as a reorientation of SOM chains into the pore space. This is consistent with the conclusions drawn for mineral soil samples [6] and peat samples [8]. Mikutta *et al.* [58] studied the hydration of polygalacturonate (PGA) coatings on alumina (Al_2O_3) and concluded from their NMR and DSC results that the PGA chains reorient into the pore space upon swelling.

Microbial Activity

Throughout the 21 days incubation the microbial activity in the investigated samples at 60 % of the maximal water holding capacity was constant and extremely low. For peat 1 it varied from 0.06 to 0.07 mg CO_2 h^{-1} 100 g^{-1} and for peat 2 from 0.08 to 0.1 mg CO_2 h^{-1} 100 g^{-1} of soil. Additional replicates of the peat samples that were fully saturated showed almost no release of CO_2 during incubation. The values of the CO_2 release from the two peats were about 100 to 1000 times smaller than reported for two mineral soil samples, where relaxation time distribution changes were significantly stronger in samples with high microbial respiratory activity [13]. Consequently, the microbial effects on the changes of relaxation time distribution of water in the two peat samples during hydration may be considered negligible.

Synthesis

The changes of the relaxation time distributions of water in the two peat samples as well as the increase of the *Q* values during hydration were most probably not caused by influences from the soil solution, internal magnetic field gradients, surface relaxivity changes or soil microorganisms and, therefore, indicate swelling of the two studied peat samples [1, 2, 6, 12, 13]. The swelling of peat was characterised by redistribution of water, by increasing amounts of non-freezable and loosely bound water, by the formation of gel phases as well as by the reduction of the translational and rotational mobility of water molecules in the two peat samples. Furthermore, swelling induced strong changes of the pore size distributions, which resulted in the reduction of number of large pores (> 50 μm) and formation of medium-sized pores (50 - 10 μm). Some time after two days of hydration the formation of small-sized pores (< 10 μm) was also observed.

It was found that the stronger volumetric swelling of peat 2 was linked to stronger changes of the pore size distribution and higher amounts of redistributed water as well as to stronger relative increases of the amounts of non-freezable and loosely bound water. In addition, more water was affected by the reduction of the translational mobility of water molecules. We suggest that this was due to the higher degradation state and the more heterogeneous matrix of peat 2. It is very likely that air drying of peat 2, previous to the rehydration, caused stronger matrix changes, such as closing of small-sized pores and collapsing of gel phases [6, 59].

The physical property of the volumetric swelling was connected to various changes of physical and physicochemical properties of peat during hydration. Stronger volumetric swelling was accompanied by stronger changes of physical and physicochemical properties of peat. The peat swelling was governed by three processes with time constants in the range of minutes (fast process), hours (medium fast process) and weeks/months (slow process) with related apparent activation energies of 5 - 50 kJ mol^{-1}, indicating the breaking of hydrogen bonds [53], water diffusion and reorientation of SOM chains during hydration [6, 38, 49].

CONCLUSIONS

The increasing amounts of non-freezable and loosely bound water as well as the reduction of the translational and rotational mobility of water molecules in the two peat samples indicate changes of the physical and physicochemical properties of the peats during swelling at constant temperature and moisture conditions. These changes took place over three time periods between minutes and months and were governed by physical and physicochemical processes. From the results we derived a mechanistic model to describe the fundamental processes of peat swelling. This model is based on results obtained from air dried peat samples with low water contents. This water exists as non-freezable water in peat. Within the first minutes after wetting of the initially water-accessible peat surfaces water structuring and water reorientation in the vicinity of the surfaces took place. This resulted in the increase of the existing non-freezable water phase due to the addition of new layers of structured water. Parallel to this process the formation of loosely bound water and gel phases occurred. Within the next following 20 to 50 hours, the swelling was mainly controlled by the diffusion of water into the peat matrix, which results in volumetric swelling and the formation of medium-sized pores (> 10 μm). After this, a very slow reorientation of SOM chains together with an ongoing volumetric swelling took place, which lasted for several months. During this time formation of medium-sized pores (> 10 μm) as well as small-sized pores (< 10 μm) occurred. Parallel to the processes which were observed during the last two time periods, intra-particulate surfaces became water-accessible which in turn resulted in the formation of non-freezable, loosely bound and gel water. The findings of this study are of environmental importance for helping to optimise renaturation and rewatering of commercially used peatlands and to better understand sorption/desorption and transport processes of pollutants and nutrients in natural organic matter rich soils.

ACKNOWLEDGEMENTS

This study was funded by the German Research Foundation, DFG, (SCH849/5-3). The T_1/T_2 - and T_2/Diffusion-correlation measurements were supported by the European Community activity Large-Scale Facility Wageningen NMR Center (FP6-2004-026164, 2006-2009). We like to thank Dr. Song from Schlumberger for the ILT programme. A special

"thank you" goes to Julia Bayer (University Koblenz-Landau) for her help in improving the manuscript.

REFERENCES

[1] Lyon WG, Rhodes DE. The swelling properties of soil organic matter and their relation to sorption of non-ionic organic compounds. cincinnati: environmental protection agency (EPA); 1991. Report No.: EPA/600/S2-91/033.

[2] Schaumann GE, Hurraß J, Müller M, Rotard W. Swelling of organic matter in soil and peat samples: insights from proton relaxation, water absorption and PAH extraction. In: Ghabbour EA, Davies G, Eds. Humic substances: nature's most versatile materials. New York: Taylor and Francis, Inc. 2004: pp. 101-17.

[3] Gaillardon P. Influence of soil moisture on long-term sorption of Diuron and Isoproturon by soil. Pestic Sci 1996; 47(4): 347-54.

[4] Johnson AC, Bettinson RJ, Williams RJ. Differentiating between physical and chemical constraints on pesticide and water movement into and out of soil aggregates. Pestic Sci 1999; 55(5): 524-30.

[5] Altfelder S, Streck T, Richter J. Effect of air-drying on sorption kinetics of the herbicide chlortoluron in soil. J Environ Qual 1999; 28: 1154-61.

[6] Todoruk TR, Langford CH, Kantzas A. Pore-scale redistribution of water during wetting of air-dried soils as studied by low-field NMR relaxometry. Environ Sci Technol 2003; 37(12): 2707-13.

[7] McBrierty VJ, Wardell GE, Keely CM, O'Neill EP, Prasad M. The characterization of water in peat. Soil Sci Soc Am J 1996; 60(4): 991-1000.

[8] McBrierty VJ, Martin SJ, Karasz FE. Understanding hydrated polymers: the perspective of NMR. J Mol Liquid 1999; 80(2,3): 179-205.

[9] Lyon WG. Swelling of peats in liquid methyl, tetramethylene and propyl sulfoxides and in liquid propyl sulfone. Environ Toxicol Chem 1995; 14(2): 229-36.

[10] Ping ZH, Nguyen QT, Chen SM, Zhou JQ, Ding YD. States of water in different hydrophilic polymers - DSC and FTIR studies. Polymer 2001; 42(20): 8461-7.

[11] Jhon MS, Andrade JD. Water and hydrogels. J Biomed Mater Res 1973; 7(6): 509-22.

[12] Schaumann GE, Hobley E, Hurraß J, Rotard W. H-NMR Relaxometry to monitor wetting and swelling kinetics in high organic matter soils. Plant Soil 2005; 275(1-2): 1-20.

[13] Jaeger F, Grohmann E, Schaumann GE. 1H NMR Relaxometry in natural humous soil samples: Insights in microbial effects on relaxation time distributions. Plant Soil 2006; 280(1-2): 209-22.

[14] Schaumann GE. Matrix relaxation and change of water state during hydration of peat. Colloids Surf A-Physicochem Eng Asp 2005; 265(1-3): 163-70.

[15] Radosta S, Schierbaum F. Polymer-water interaction of maltodextrins. Part III: non-freezable water in maltodextrin solutions and gels. Starch - Stärke 1990; 42(4): 142-7.

[16] Yoshida H, Hatakeyama T, Hatakeyama H. Characterization of water in polysaccharide hydrogels by DSC. J Thermal Anal 1993; 40(2): 483-9.

[17] Radosta S, Schierbaum F, Yuriev WP. Polymer-water interaction of maltodextrins. Part II: NMR study of bound water in liquid maltodextrin-water systems. Starch - Stärke 1989; 41(11): 428-30.

[18] Bayer JV, Jaeger F, Schaumann GE. Proton Nuclear magnetic resonance (NMR) relaxometry in soil science applications. Open Magn Reson J 2010 (accepted).

[19] Jaeger F, Rudolph N, Lang F, Schaumann GE. Effects of soil solution's constituents on proton NMR relaxometry of soil samples. Soil Sci Soc Am J 2008; 72(12): 1694-707.

[20] Keating K, Knight R. A laboratory study to determine the effect of iron oxides on proton NMR measurements. Geophysics 2007; 72(1): E27-32.

[21] Fyfe CA, Blazek AI. Investigation of hydrogel formation from hydroxypropylmethylcellulose (HPMC) by NMR spectroscopy and NMR imaging techniques. Macromolecules 1997; 30(20): 6230-7.

[22] Carenza M, Cojazzi G, Bracci B, *et al.* The state of water in thermoresponsive poly(acryloyl-L-proline methyl ester) hydrogels observed by DSC and 1H-NMR relaxometry. Radiat Phys Chem 1999; 55(2): 209-18.

[23] Callaghan PT, Jolley KW, Lelievre J, Wong RBK. Nuclear magnetic resonance studies of wheat starch pastes. J Colloid Interface Sci 1983; 92(2): 332-7.

[24] Kleinberg RL, Straley C, Kenyon WE, Akkurt R, Farooqui SA. Nuclear magnetic resonance of rocks: T1 *vs*. T2. Society of Petroleum Engineers 1993; 68th Annual Technical Conference and Exhibition of the Society of Petroleum Engineers, 1993; pp. 553-63. Houston: Texas.

[25] Packer KJ, Dick DAT, Wilkie DR. The dynamics of water in heterogeneous systems. Philos Trans R Soc Lond B Biol Sci 1977; 278(959): 59-87.

[26] Pouliquen D, Gallois Y. Physicochemical properties of structured water in human albumin and gammaglobulin solutions. Biochimie 2001; 83(9): 891-8.

[27] Pouliquen D, Omnes M-H, Seguin F, Gaignon J-L. Changes in the dynamics of structured water and metabolite contents in early developing stages of eggs of turbot (Psetta maxima). Comp Biochem Physiol A 1998; 120(4): 715-26.

[28] Dunn K-J, Bergman DJ, Latorraca GA. Handbook of geographical exploration-seismic exploration: nuclear magnetic resonance-petrophysical and logging applications. 1st ed. Oxford: Pergamon 2002.

[29] Kleinberg RL. Nuclear magnetic resonance. In: Wong P-Z, Ed. Methods in the physics of porous media. San Diego: Academic Press 1999; pp. 337-85.

[30] Bird NRA, Preston AR, Randall EW, Whalley WR, Whitmore AP. Measurement of the size distribution of water-filled pores at different matric potentials by stray field nuclear magnetic resonance. Eur J Soil Sci 2005; 56(1): 135-43.

[31] Brownstein KR, Tarr CE. Importance of classical diffusion in NMR studies of water in biological cells. Phys Rev A 1979; 19(6): 2446-53.

[32] Godefroy S, Korb JP, Fleury M, Bryant RG. Surface nuclear magnetic relaxation and dynamics of water and oil in macroporous media. Phys Rev E 2001; 64(2-1): 021605.

[33] Kenyon WE, Kolleeny JA. NMR surface relaxivity of calcite with adsorbed Mn^{2+}. J Colloid Interface Sci 1995; 170(2): 502-14.

[34] Bryar TR, Daughney CJ, Knight RJ. Paramagnetic effects of iron(III) species on nuclear magnetic relaxation of fluid protons in porous media. J Magn Reson 2000; 142(1): 74-85.

[35] Meiboom S, Gill D. Modified spin-echo method for measuring nuclear relaxation times. Rev Sci Instrum 1958; 29: 688-91.

[36] Roberts SP, Macdonald PJ, Tritchard T. A bulk and spatioal resolved NMR relaxation study of sandstone rock plugs. J Magn Reson A 1995; 116: 189-95.

[37] Jaeger F, Bowe S, Schaumann GE. Evaluation of 1H NMR relaxometry for the assessment of pore size distribution in soil samples. Eur J Soil Sci 2009; 60(6): 1052-64.

[38] Diehl D, Schaumann GE. Wetting mechanism assessed from time dependent sessile drop shape. Hydrol Process 2007; 21(17): 2255 - 65.

[39] Veevaete M. Applications of Earth's Field NMR to porous systems and polymer gels. Bremen, Germany: University of Bremen 2008.

[40] Butler JP, Reeds JA, Dawson SV. Estimating solutions of first kind integral equations with nonnegative constraints and optimal smoothing. SIAM J Numer Anal 1981; 18(3): 381-97.

[41] van Dusschoten D, Moonen CT, de Jager PA, Van As H. Unraveling diffusion constants in biological tissue by combining Carr-Purcell-Meiboom-Gill imaging and pulsed field gradient NMR. Magn Reson Med 1996; 36(6): 907-13.

[42] Song YQ, Venkataramanan L, Hürlimann MD, Flaum M, Frulla P, Straley C. T1-T2 correlation spectra obtained using a fast two-dimensional laplace inversion. J Magn Reson 2002; 154(2): 261-8.

[43] Hurlimann MD, Venkataramanan L, Flaum C. The diffusion-spin relaxation time distribution function as an experimental probe to characterize fluid mixtures in porous media. J Chem Phys 2002; 117(22): 10223-32.

[44] Venkataramanan L, Song YQ, Hürlimann MD. Solving Fredholm integrals of the first kind with tensor productstructure in 2 and 2.5 dimensions. IEEE Trans Signal Proces 2002; 50: 1017-26.

[45] Hahn EL. Spin echoes. Phys Rev 1950; 80(4): 580-94.

[46] Valckenborg R. NMR on technological porous materials. Eindhoven, The Netherlands: Eindhoven University of Technology 2001.

[47] Nordgren A. Apparatus for the continuous, long-term monitoring of soil respiration rate in large numbers of samples. Soil Biol Biochem 1988; 20(6): 955-7.

[48] Wedler G. Lehrbuch der physikalischen Chemie. 3rd ed. Weinheim: VCH Verlagsgesellschaft mbH 1987.

[49] Sparks DL. Kinetics of ionic reactions in clay minerals and soils. Adv Agron 1985; 38: 231-66.
[50] Delville A, Letellier M. Structure and dynamics of simple liquids in heterogeneous condition: an NMR study of the clay - water interface. Langmuir 1995; 11(4): 1361-7.
[51] Kinniburgh DG, Miles DL. Exraction and chemical analysis of interstitial water from soils and rocks. Environ Sci Technol 1983; 17: 362-8.
[52] Wynne-Jones S, Blanshard JMV. Hydration studies of wheat starch, amylopectin, amylose gels and bread by proton magnetic resonance. Carbohydr Polym 1986; 6(4): 289-306.
[53] Smith JD, Cappa CD, Wilson KR, Messer BM, Cohen RC, Saykally RJ. Energetics of hydrogen bond network rearrangements in liquid water. Science 2004; 306(5697): 851-3.
[54] Holz M, Heila SR, Saccob A. Temperature-dependent self-diffusion coefficients of water and six selected molecular liquids for calibration in accurate 1H NMR PFG measurements. Phys Chem Chem Phys 2000; 2(20): 4740-2.
[55] Mitra PP, Sen PN, Schwartz LM. Short-time behavior of the diffusion coefficient as a geometrical probe of porous media. Phys Rev B 1993; 47(14): 8565-74.
[56] Beuling EE, Van Dusschoten D, Lens P, Van Den Heuvel JC, Van As H, Ottengraf SPP. Characterization of the diffusive properties of biofilms using pulsed field gradient-nuclear magnetic resonance. Biotechnol Bioeng 1998; 60(3): 283-91.
[57] Liu WG, Yao KD. What causes the unfrozen water in polymers: hydrogen bonds between water and polymer chains? Polymer 2001; 42(8): 3943-7.
[58] Mikutta C, Krüger J, Schaumann GE, Lang F. Restructuring of polygalacturonate on alumina upon hydration - effect on phosphate sorption kinetics. Geochim Cosmochim Acta 2006; 70(12): 2957-69.
[59] Todoruk TR, Litvina M, Kantzas A, Langford CH. Low-field NMR relaxometry: a study of interactions of water with water-repellant soils. Environ Sci Technol 2003; 37(12): 2878-82.

Received: July 26, 2009 Revised: November 30, 2009 Accepted: December 04, 2009